1-1-1996

An O(N) Algorithm for Stokes and Laplace Interactions of Particles

Ashok S. Sangani
Syracuse University

Guobiao Mo
Syracuse University

An O(N) algorithm for Stokes and Laplace interactions of particles

Ashok S. Sangani and Guobiao Mo

Citation: Phys. Fluids **8**, 1990 (1996); doi: 10.1063/1.869003
View online: http://dx.doi.org/10.1063/1.869003
View Table of Contents: http://pof.aip.org/resource/1/PHFLE6/v8/i8
Published by the American Institute of Physics.

An $O(N)$ algorithm for Stokes and Laplace interactions of particles

Ashok S. Sangani[a] and Guobiao Mo
Department of Chemical Engineering and Materials Science, Syracuse University, Syracuse, New York 13244

(Received 27 December 1995; accepted 12 April 1996)

A method for computing Laplace and Stokes interactions among N spherical particles arbitrarily placed in a unit cell of a periodic array is described. The method is based on an algorithm by Greengard and Rokhlin [J. Comput. Phys. **73**, 325 (1987)] for rapidly summing the Laplace interactions among particles by organizing the particles into a number of different groups of varying sizes. The far-field induced by each group of particles is expressed by a multipole expansion technique into an equivalent field with its singularities at the center of the group. The resulting computational effort increases only linearly with N. The method is applied to a number of problems in suspension mechanics with the goal of assessing the efficiency and the potential usefulness of the method in studying dynamics of large systems. It is shown that reasonably accurate results for the interaction forces are obtained in most cases even with relatively low-order multipole expansions.
 [S1070-6631(96)01108-7]

I. INTRODUCTION

Numerical simulations of motion of particles through a suspending fluid provide valuable insight into the complex interrelationship between the microscale physics, the microstructure, and the macroscopic behavior of suspensions. However, the problem of determining hydrodynamic interactions among many particles is computationally intensive with most of the existing methods for simulations suitable only for a relatively small number of interacting particles, typically of $O(100)$. While this is adequate for many problems, there are also large numbers of problems for which it is desirable to simulate systems containing much greater number of particles. For example, the uniform state of small Reynolds number, finite Stokes number, gas-solid fluidized bed is known to be unstable for certain ranges of its parameters (the volume fraction of the particles and the Stokes number) resulting in the formation of large bubbles or regions devoid of particles. Large-scale simulations are needed to understand in detail the mechanisms responsible for these macroscopic instabilities. Similarly, problems involving concentrated fiber suspensions with nl^3 of $O(10^2-10^3)$ require large-scale simulations involving thousands of fibers in order that the box size used in the simulations does not significantly affect the behavior of such suspensions. Here, n is the number density of fibers and l is the length of fibers. Moreover, recent experimental and numerical work on sedimenting fibers suggest that the uniform state of such suspensions is unstable resulting in the formation of clusters.[1] Large-scale simulations are needed to determine the cluster size distribution and the resulting properties of the sedimenting fiber suspensions. Large-scale simulations are also needed in the study of suspensions with significant wall effects, polydisperse suspensions, or for suspensions in which the hydrodynamic interactions are expected to be screened at distances large compared to the size of the particles.

Two major difficulties in computing hydrodynamic interactions among particles in Stokes (small Reynolds number) flow are: (i) the long-range, multiparticle nature of interactions; and (ii) the lubrication effects arising from a relative motion of particles in close proximity to each other. These are explained in more detail below.

The velocity disturbance caused by a particle with a net nonzero force acting on it decays only as $1/r$, r being the distance from the center of the particle, and therefore it is not possible to use an arbitrary cut-off radius for truncating the hydrodynamic interactions among particles. In other words, one must compute the interactions among *all* the particles in the suspension. The velocity induced by a particle is generally expressed in terms of a distribution of hydrodynamic force density acting along its surface. The multiparticle nature of the interaction arises due to the fact that this force density is unknown and is to be determined as a part of the solution by solving for the force density on all the particles simultaneously. This is different, for example, from the problem of computing Coulombic interactions among species with known charges for which the interactions are also long-ranged but, because the charge on the individual species is known, the interactions are pair-additive. As a consequence, no simple pair-additive approximation can be made in computing hydrodynamic interactions.

When two particles in close proximity approach toward each other with an $O(1)$ relative velocity, the fluid in the gap between the particles must squeeze out radially from the narrow gap between the particles. This results in a radial velocity of $O(\epsilon^{-1/2})$ in the gap region of thickness ϵ and a force density of $O(\epsilon^{-2})$ localized to an $O(\epsilon)$ surface area of each particle. This is known as the lubrication effect. (See, for

[a] Electronic mail: asangani@mailbox.syr.edu

 1070-6631/96/8(8)/1990/21/$10.00

example, Happel and Brenner[2] or Kim and Karrila[3] for details.) Since the lubrication force density is highly localized to a relatively small area of the the surface of the particles, the conventional numerical techniques, such as the boundary integral technique in which the surface of the particles is discretized into a number of surface elements (see Pozrikidis[4] for details), become impractical for large systems as the number of discretized elements needed for resolving the lubrication effects become prohibitively large as the two particles approach each other.

To overcome the above two difficulties, Brady and Bossis[5] devised an ingenious scheme in which the many-particle resistivity matrix, which gives the force density on the particles given their velocities, is expressed as a sum of far-field approximation to the many-particle mobility matrix inverse and the pair resistivity tensors. The former accounts for the long-range, multiparticle nature of the interactions while the latter accounts for the lubrication forces between pairs of particles which contribute in a pair-additive manner to the resistivity tensor. This method is also used by Ladd[6] who showed that the approximation devised by Brady and Bossis can be systematically improved by including higher-order approximations to the far-field mobility matrix. The main advantage of the method over the conventional boundary integral method is that relatively few unknowns (typically 11 to 26) per particle are needed for determining many-particle interactions with an accuracy that is adequate for many dynamic simulation problems.[5,6] Unfortunately, the method requires inverting a far-field mobility matrix with at least $(11N)^2$ elements, the computational effort for which grows as N^2 as the system size increases, N being the number of particles in the system. This limits the computations to N of no more than few hundreds.

Alternate methods that do not require inverting the mobility matrix have been proposed by Mo and Sangani,[7] Sangani and Mo,[8] and Cichoki *et al.*[9] Cichoki *et al.* employed the same idea as Brady and Bossis to account for the lubrication effects but avoided the matrix inversion with the help of a suitable transformation of the equations governing the multipoles. In the present study we use the method proposed by Sangani and Mo. According to this method, the force density on the particles is decomposed first into a lubrication force density which is localized to the gap region between the closely spaced particles and a regular force density which is distributed on the entire surface of the particles. The velocity due to the latter is expressed in terms of force multipoles at the center of the particles while that due to the former is approximated in terms of a force dipole at the center of the gap between the particles. This method thus accounts for both the long-range, multiparticle nature of the interactions and the lubrication effects. Application of the boundary conditions on the surface of the particles leads to a system of linear equations of the form $\mathbf{A}\cdot\mathbf{x}=\mathbf{b}$, where $\mathbf{x}$ is a vector of translational and rotational velocity of the particles and the induced force multipoles, $\mathbf{A}$ is an $O(N\times N)$ matrix and $\mathbf{b}$ is a vector that depends on the imposed flow. In Sangani and Mo,[8] each element of the matrix $\mathbf{A}$ was evaluated separately and the resulting equations were solved subsequently to determine the force multipoles and the velocities of the particles. The accuracy of the method was shown to be comparable to that of the method of Brady and Bossis.[5] However, since each element of $\mathbf{A}$ was evaluated separately, the method also required $O(N^2)$ computations, and, consequently, no significant computational savings resulted even though it avoided the computation of the mobility matrix inverse.

For large systems, it will be advantageous to devise schemes in which the computational effort increases much more slowly with N. The solution of the set of linear equations $\mathbf{A}\cdot\mathbf{x}=\mathbf{b}$ is typically obtained by iterative methods when N is large. In order that this can be accomplished with only an $O(N)$ computational effort, one must be able to compute $\mathbf{A}\cdot\mathbf{x}$ for a given $\mathbf{x}$ in an $O(N)$ time. This is the main objective of the present investigation. Our method is based on a fast summation technique based on hierarchial grouping of particles developed for computing Coulombic and gravitational interactions. There are several ways of doing this (see, for example, Apple,[10] Barnes and Hut,[11] and Greengard and Rokhlin.[12]) Here, we shall follow the approach outlined by Greengard and Rokhlin.[12] These investigators (and the other co-workers of Greengard) have developed an algorithm for computing Laplace and Coulombic interactions in the two- as well as three-dimensional space[13,14] and for the elastic interactions in the two-dimensional space.[15] The field created by a group of particles far from a given particle is expressed in terms of multipoles at the center of the group as described in more detail later in this paper. Since the field represented by a group of particles with a fixed number of multipoles becomes accurate when the distance from the center of the group is large compared with the linear dimension of the group size, we need a hierarchy of groups in which the field felt by a given particle is evaluated by using smaller groups of particles that are relatively close to the particle and larger groups of particles that are further away from it.

The method described by Greengard and Rokhlin for solving Laplace equation starts with a discretization of the boundary integrals and this makes it somewhat inefficient for treating suspension problems in which the lubrication forces are significant. Although the computational effort scales linearly with N, the number of discretization elements per particles will be prohibitively large when the lubrication effects are significant. However, by combining their technique of rapidly summing the interactions with the method of Sangani and Mo,[8] in which the number of unknowns per particle is small due to explicit treatment of the lubrication effect, it should be possible to decrease the overall computational effort significantly. Also, as we shall see, the extension of the method to sum Stokesian interactions is nontrivial. The method requires developing appropriate expressions for the far-field and near-field representations of the field induced by a group of particles. Greengard and Rokhlin gave these expressions for the Laplace equation and the present study derives similar relations for the Stokes equations. The method is applied to several problems to assess the efficiency and the potential usefulness of the algorithm.

We should perhaps mention here about an $O(N)$ algorithm based on the lattice-Boltzmann gas technique that already exists for the study of hydrodynamic interactions in

suspensions. The fluid continuum in Stokes interactions is replaced by a lattice-Boltzmann gas with appropriate rules for its molecules to exchange their positions and momentum. It is found that with suitable rules for this exchange in the bulk and at the interface between the particles and the molecules of the lattice-Boltzmann gas, it is possible to mimic the behavior of rigid particles suspended in a Navier–Stokes flow. A method based on this idea has been extensively tested in two recent papers by Ladd.[16,17] Ladd has been able to carry out Stokesian dynamic simulations of suspensions with N of $O(10^4)$ using this technique. In addition to being $O(N)$ in computations, the method has the advantage of being able to treat both the nonzero Reynolds number flows past fixed particles and the suspensions of submicron sized particles for which the Brownian forces are significant. This method, however, is still in its early stages of development with its accuracy and efficiency for large N systems untested and unchallenged by the other direct approaches based on solving partial differential equations arising from the continuum approximation. It is hoped that in the least the method developed here may serve as a check and an alternate to the lattice-Boltzmann gas based algorithms for monodisperse suspensions of rigid particles. Furthermore, since the size of the lattice is typically governed by the smallest dimension of the particles, it appears that the method of summing interactions by hierarchial grouping will be far more efficient in dealing with the suspensions of slender fibers or polydisperse suspensions. Also, since in general, it is a nontrivial task to determine the appropriate rules for the exchange of momentum at the interface to mimic boundary conditions other than the no-slip condition, it is expected that the method described in this paper will be more readily adapted to the suspensions of charged particles,[18] drops or bubbles.[7] Note that for highly deformable particles and slender fibers, the interactions can be computed using the integral equation representation for the Stokes flow instead of the multipole representation. The lubrication effect mentioned earlier is likely to play less important a role for these cases, and consequently the straightforward integral equation coupled with the fast summation method described here is expected to be adequate for the study of such suspensions.

The basic method is outlined in Sec. II where we consider a simple case of Laplace interactions. We have chosen to treat these interactions first since the method is much easier to understand for this case and because of its application to the simulations of bubbly liquids at large Reynolds and small Weber numbers (see Sangani and Didwania[19]). Although the general principles are the same as in the method outlined by Greengard and Rokhlin, the details are quite different. In Sec. III we describe the method for computing Stokes interactions. In Sec. IV we assess the efficiency of the algorithm by applying it to a number of problems. First we consider two Laplace interaction problems: (i) determination of the effective reaction rate constant in a diffusion-limited reacting medium; and (ii) determination of the added mass coefficient for particles in inviscid suspensions. Next, we consider three Stokes flow interaction problems: (i) a uniform flow through fixed beds of particles; (ii) effective viscosity of suspensions; and (iii) sedimentation velocity and hydrodynamic fluctuations in suspensions.

II. THE METHOD FOR LAPLACE INTERACTIONS

As mentioned in Sec. I, we shall first consider a simpler problem of determining Laplace interactions of spherical particles. We shall explain the method in reference to a problem of diffusion-controlled reactions. This will be applicable with minor modifications to the other problems of Laplace interactions.

When the size of one of the reactant species is much greater than the other, the larger species may essentially be regarded as immobile and the rate of reaction then depends on the rate at which the smaller species diffuses through the medium and arrives at the surface of the larger, immobile species. To model this situation, we consider a suspension consisting of N spherical particles each of radius a placed within a unit cell of a periodic array. The suspending fluid contains a species with a linear dimension much smaller than a which diffuses through the fluid with a constant diffusivity D. The species reacts very rapidly with the spheres such that its concentration at the surface of the spheres may be taken to be vanishingly small. We shall assume that the species is continuously produced in the fluid at a constant rate throughout the fluid medium. At steady state the average concentration $\langle C\rangle$ of the species in the suspension is determined by the balance between the rate at which it is produced in the bulk and the rate at which it is consumed by the reaction. The problem then is to determine the non-dimensional reaction rate constant R_s defined by

$$\langle Q\rangle = 4\pi a D R_s \langle C\rangle. \tag{1}$$

Here, $\langle Q\rangle$ is the average quantity of the species reacting per unit time on a single sphere. When ϕ, the volume fraction of the spheres, is small, the interactions among spheres can be neglected, and $R_s = 1$—a result first given by Smoluchowski.[20] An estimate of the first correction for small but finite ϕ was given by Felderhof and Deutch,[21] and, more recently, numerical simulations have been used to compute R_s as a function of ϕ for dense suspensions (see, for example, Felderhof[22]). Our goal will be to calculate R_s for a few selected configurations of N spheres. The fluid is assumed to be at rest so that the species concentration C satisfies the Poisson equation

$$\nabla^2 C + S = 0 \tag{2}$$

with the boundary condition $C = 0$ on the surface of the spheres. Here, DS is the net rate at which the species is produced per unit volume of the fluid and is related to $\langle Q\rangle$ by $DS(1-\phi) = n\langle Q\rangle$, n being the number density of the spheres. It may be noted that the presence of S in Eq. (2) renders it a Poisson equation instead of the Laplace equation but we shall continue to refer to the interactions as Laplacian since Eq. (2) is a rather trivial special case of the more general Poisson equation in which the sink term is a function of the position. In Sec. IV, where we present the results of computations for R_s, we shall also consider the problem of

added mass whose governing differential equation is indeed the Laplace equation, and the solution for that case will be obtained simply by setting $S=0$.

A. A review of an $O(N^2)$ algorithm

Before describing the $O(N)$ algorithm in detail, it is useful to present a more conventional method of multipole expansion in which the computations grow as N^2 as the system size is increased. The method has a close connection to the boundary integral method but enjoys an advantage of a faster convergence for simple particle shapes such as spheres considered in the present study. This method was outlined in reference to the problem of determining the effective thermal conductivity and the added mass coefficient for a given configuration of spheres in our earlier studies.[23,24]

The concentration C of the diffusing species can be expressed in terms of the Green's function (or the fundamental singular solution) S_1 of the Poisson equation as

$$C(\mathbf{x})=C^{\infty}+\sum_{\alpha=1}^{N}\mathscr{G}^{\alpha}S_1(\mathbf{x}-\mathbf{x}^{\alpha}), \tag{3}$$

where C^{∞} is to be chosen such that the average concentration equals $\langle C\rangle$, $\mathscr{G}^{\alpha}$ is a differential operator that will be defined more precisely later in the section, $\mathbf{x}^{\alpha}$ is the center of the particle α, and S_1 is the spatially periodic Green's function satisfying

$$\nabla^2 S_1(\mathbf{x})=4\pi\left[\tau^{-1}-\sum_{\mathbf{x_L}}\delta(\mathbf{x}-\mathbf{x_L})\right]. \tag{4}$$

Here, $\mathbf{x_L}$ represents the lattice points of the periodic array, τ is the volume of the unit cell of the periodic array, and δ is the Dirac's delta function. The constant sink term τ^{-1} in the above expression is needed to balance the source term at the lattice points. An Ewald technique for evaluating S_1 is described in detail by Hasimoto.[25] More details including expressions for the derivatives of S_1 are given in Sangani *et al.*[24] and Cichoki and Felderhof.[26] As shown by Hasimoto, $S_1(\mathbf{x})$ has a singular, source-like, behavior near lattice points where it behaves as $1/|\mathbf{x}-\mathbf{x_L}|$.

The use of spatially periodic Green's function ensures that the field induced by each particle, i.e., $\mathscr{G}^{\alpha}S_1(\mathbf{x}-\mathbf{x}^{\alpha})$, is spatially periodic, and hence consistent with the imposed periodic boundary condition. Thus, we only need to satisfy the boundary condition at the surface of the particles. For the case of spherical particles it is convenient to express C near each particle in terms of spherical harmonics in a polar coordinate system with its origin at the center of that particle. Thus, near particle α, we express C as

$$C=-Sr^2/6+\sum_{i=0}^{1}\sum_{n=0}^{\infty}\sum_{m=0}^{n}[E_{nm}^{i,\alpha}+A_{nm}^{i,\alpha}r^{-2n-1}]Y_{nm}^{i}(\mathbf{r}), \tag{5}$$

where $\mathbf{r}=\mathbf{x}-\mathbf{x}^{\alpha}$, and Y_{nm}^{i} are the solid spherical harmonics with

$$Y_{nm}^{0}=r^n P_n^m(\mu)\cos m\varphi, \quad Y_{nm}^{1}=r^n P_n^m(\mu)\sin m\varphi. \tag{6}$$

Here, $\mu=\cos\theta$ and the spherical polar angles θ and φ are defined by $r_1=r\cos\theta$, $r_2=r\sin\theta\cos\varphi$, and $r_3=r\sin\theta\sin\varphi$. Now the boundary condition of vanishing C at $r=a$ yields

$$E_{nm}^{i,\alpha}+a^{-2n-1}A_{nm}^{i,\alpha}-\frac{1}{6}Sa^2\delta_{n0}\delta_{m0}\delta_{i0}=0, \tag{7}$$

where δ_{n0} is a Kronecker delta function whose value is unity for $n=0$ and zero otherwise.

In order that Eq. (3) can be recast into Eq. (5), we define the differential operator $\mathscr{G}^{\alpha}$ such that the singular terms at $\mathbf{x}^{\alpha}$ in Eq. (3) are exactly the same as those in Eq. (5). Since the singular part of S_1 equals $1/r$, we require that

$$\mathscr{G}^{\alpha}r^{-1}\equiv\sum_{i,n,m}r^{-2n-1}A_{nm}^{i,\alpha}Y_{nm}^{i}, \tag{8}$$

where the summation over i,n,m is the same as that in Eq. (5). In Appendix A, we have compiled a number of useful results on the differentiation of $1/r$ and the other spherical harmonics. Using Eq. (A1), we see at once that

$$\mathscr{G}^{\alpha}=\sum_{i,n,m}\lambda_{nm}^{-1}A_{nm}^{i,\alpha}\mathscr{D}_{nm}^{i}, \tag{9}$$

where λ_{nm} is given by Eq. (A2) and $\mathscr{D}_{nm}^{i}$ is the differential operator defined by Eq. (A3). The constant $A_{nm}^{i,\alpha}$ will be referred to as the induced multipoles.

Now the coefficients $E_{nm}^{i,\alpha}$ of the terms that are regular at $r=0$ in Eq. (5) are related to the nth order derivatives of the regular part of C at $r=0$ by [cf. Eqs. (A6)-(A8)]

$$E_{nm}^{i,\alpha}=\epsilon_{nm}[\mathscr{D}_{nm}^{i}(C^{\mathrm{reg}}+Sr^2/6)]_{r=0}, \tag{10}$$

where ϵ_{nm} is given by Eq. (A8) and C^{reg} equals C minus the singular part at $r=0$, i.e. $C^{\mathrm{reg}}=C-\mathscr{G}^{\alpha}r^{-1}$. Substituting for $\mathscr{G}^{\alpha}$ from Eq. (9) into Eq. (3) and combining it with Eq. (10) yields

$$E_{nm}^{i,\alpha}=\epsilon_{nm}\Bigg[\{\mathscr{D}_{nm}^{i}(C^{\infty}+Sr^2/6)\}_{r=0}+\sum_{k=0}^{\infty}\sum_{l=0}^{k}\sum_{j=0}^{1}\sum_{\gamma=1}^{N}\lambda_{kl}^{-1}A_{kl}^{j,\gamma}\mathscr{D}_{nm}^{i}\mathscr{D}_{kl}^{j}S_1(\mathbf{x}^{\alpha}-\mathbf{x}^{\gamma})\Bigg], \tag{11}$$

where the singular part $1/r$ must be removed from S_1 before differentiating it for $\gamma=\alpha$. For later reference, we note that S is related to the sum of monopoles by means of a simple relation

$$S=-\frac{4\pi}{\tau}\sum_{\gamma=1}^{N}A_{00}^{0,\gamma} \tag{12}$$

obtained by combining Eqs. (4) and (9). Here, we made use of the fact that all singularities are situated inside the particles so that, for a point lying in the fluid, Eq. (4) simplifies to $\nabla^2 S_1=4\pi/\tau$.

Now the $O(N^2)$ algorithm consists of truncating the infinite set of equations represented by Eqs. (7) and (11) by considering only the equations and multipoles $A_{nm}^{i,\alpha}$ with $n\leq N_s$. This results in a total of $N_t=N(N_s+1)^2$ number of equations in an equal number of unknown multipoles $A_{kl}^{i,\gamma}$. These equations are cast into a form $\mathbf{A}\cdot\mathbf{x}=\mathbf{b}$ where $\mathbf{x}$ is an

N_t-vector of unknown multipole strengths, $\mathbf{A}$ is an $N_t \times N_t$ matrix whose coefficients are the derivatives of $S_1(\mathbf{x}^\alpha - \mathbf{x}^\gamma)$, and $\mathbf{b}$ is an N_t-vector that is related to C^∞, or, equivalently, $\langle C \rangle$. The computational cost is typically governed by the calculation of N_t^2 elements of the matrix $\mathbf{A}$. This is computationally intensive since S_1 itself is to be computed using series in real and reciprocal space lattice vectors.[25] When high accuracy in numerical simulations is not critically required, it is possible to avoid the repeated calculations of S_1 for all pairs of particles by using a grid interpolation scheme in which the unit cell is first divided into a number of smaller cubes with the help of a grid and all the derivatives of S_1 needed in the calculations are evaluated at the grid points and stored for the interpolation purpose in the subsequent calculations. Although this reduces the computational effort considerably, the computations still grow quadratically with N_t.

The set of linear algebraic equations is subsequently solved using an appropriate iterative solver and this requires computations of $O(N_t^2)$ times the number of iterations required for the convergence to within a desired accuracy. Thus, the overall computational effort and the memory storage (for the matrix $\mathbf{A}$) scale as N_t^2. [In earlier calculations,[8,24] we solved the system of equations using a Gaussian elimination algorithm which required an $O(N_t^3)$ effort, but for small N, the computational time was mostly governed by the time for computing the matrix elements and thus this step was not crucial.]

B. Far- and near-field representations of the disturbances induced by a group of particles

In order that the overall computations for determining the multipoles scale linearly with N_t, we must be able to determine $E_{nm}^{i,\alpha}$ with $O(N_t)$ computations. The method described in Sec. II A is inefficient for large N_t since it computes the disturbance created by each particle γ separately at the center of each particle α. Clearly, the field created by particles that are separated by a large distance from particle α can be grouped together for the purpose of evaluating their effect on particle α. Similarly, all the particles near α feel similar regular field (C^{reg}) from the group of particles far away from them and therefore the calculation of the regular fields for the particles could also be grouped together. If we simply create all the groups of particles with each group containing nearly an equal number P of particles, then we would require $O((N/P)^2)$ group–group interaction computations. In addition, we must separately account for the interactions among particles that are neighbors and this would require $O(NP)$ computations resulting in a total computational effort that scales roughly as $N^2/P^2 + NP$. This has a minimum for $P = O(N^{1/3})$, and the total computational time for this optimum P scales as $N^{4/3}$.

In order to further reduce the order of computations we must create a hierarchy among groups of particles and adopt a strategy in which the regular field near particle α is evaluated by combining greater number of particles that are further away from it and fewer particles that are closer to it. This can be accomplished using the algorithm of Greengard and Rokhlin[12] which we shall present in more detail in Sec. II C. Here, we shall derive the expressions that are needed for combining the fields induced by a group of particles and the regular fields ''felt'' by a group of particles. In particular, we need to know (i) how to translate a field induced due to a singularity at $\mathbf{x}^c$ to a field with singularity at another point $\mathbf{x}^p$ such that both fields are identical at a point $\mathbf{x}$ sufficiently far away from both $\mathbf{x}^c$ and $\mathbf{x}^p$; and (ii) how to translate a field which is regular and expressed in solid spherical harmonics at one point to a regular field expanded around another point in its vicinity. The first one will be useful, for example, in combining the fields induced by a group of particles γ while the second one will be useful in determining C^{reg} around a number of particles near α. Greengard and Rokhlin accomplished these two tasks through the use of addition theorems for Legendre functions. We shall use a different procedure here, one that we have found more suitable to treat the case of Stokes flow to be considered in Sec. III. Also, since the method presented here incorporates the periodic boundary conditions imposed by the presence of the unit cell at the outset, it has the advantage of dealing more easily with various kinds of non-absolutely convergent sums that otherwise arise in calculations involving the Green's function for infinite domains. The case of interactions among finite number of particles in an infinite medium can of course be trivially recovered by substituting $1/r$ in place of $S_1(r)$.

1. Translation of singularities

We wish to translate a field $C^c \equiv \mathscr{G}^c S_1(\mathbf{x} - \mathbf{x}^c)$ with its singularities at $\mathbf{x}^c$ to an equivalent field C^p with its singularities at $\mathbf{x}^p$ such that both C^c and C^p give the same value of C or its derivatives at a point $\mathbf{x}$ far from both $\mathbf{x}^c$ and $\mathbf{x}^p$. We start with a Green's identity

$$\int_V (f\nabla^2 C - C\nabla^2 f)\, dV_{\mathbf{r}} = \int_{\partial V} (f\nabla C - C\nabla f)\cdot \mathbf{n}\, dA_{\mathbf{r}}, \quad (13)$$

where V is any volume enclosing points $\mathbf{x}^c$ and $\mathbf{x}^p$, ∂V is its surface, $\mathbf{n}$ is the unit outward normal on ∂V, and $\mathbf{r} = \mathbf{x} - \mathbf{x}^p$. Now we choose f to equal $Y_{nm}^j(\mathbf{r})$ ($j = 0,1$) and substitute in turn for C both C^c and C^p. Since $C^c = C^p$ and $\nabla C^c = \nabla C^p$ on ∂V, the surface integrals in both must be equal and therefore we obtain

$$\int_V Y_{nm}^j(\mathbf{r})\nabla^2 C^c\, dV_{\mathbf{r}} = \int_V Y_{nm}^j(\mathbf{r})\nabla^2 C^p\, dV_{\mathbf{r}}, \quad (14)$$

where we have made use of the fact that $\nabla^2 f = \nabla^2 Y_{nm}^j(\mathbf{r}) = 0$. (Note that this does not assume that C^c and C^p are equal at all points within V, only their equivalence on ∂V.) Care must be taken in evaluating the above integrals since the Laplacian of C^c or C^p is a series in generalized functions

$$\nabla^2 C^c \equiv \mathscr{G}^c \nabla^2 S_1(\mathbf{r} - \mathbf{r}^{cp}) = 4\pi \left[A_{00}^{0,c}\tau^{-1} - \sum_{i,k,l} \lambda_{kl}^{-1} A_{kl}^{i,c} \mathscr{D}_{kl}^i \delta(\mathbf{r} - \mathbf{r}^{cp}) \right], \quad (15)$$

where $\mathbf{r}^{cp}=\mathbf{x}^c-\mathbf{x}^p$. Here, we have used Eq. (9) to represent C^c in terms of multipoles $A_{kl}^{i,c}$ at $\mathbf{x}^c$ and Eq. (4) for the Laplacian of S_1, the points $\mathbf{x}^c$ and $\mathbf{x}^p$ being assumed to lie inside the basic unit cell with $\mathbf{x_L}=\mathbf{0}$.

Now since C^p must be spatially periodic, the most general form for it with singularities at $\mathbf{x}^p$ is

$$C^p=e^p+\sum_{i,k,l}\lambda_{kl}^{-1}A_{kl}^{i,p}\mathscr{D}_{kl}^{i}S_1(\mathbf{r}), \tag{16}$$

where e^p is a constant that may arise in translating the singularities from $\mathbf{x}^c$ to $\mathbf{x}^p$, and $A_{kl}^{i,p}$ are the multipoles at $\mathbf{x}^p$. Substituting Eqs. (15) and (16) into Eq. (14) we obtain

$$(-1)^n A_{nm}^{j,p}=\lambda_{nm}\epsilon_{nm}\sum_{i,k,l}(-1)^k\lambda_{kl}^{-1}A_{kl}^{i,c}\mathscr{D}_{kl}^{i}Y_{nm}^{j}(\mathbf{r}^{cp}). \tag{17}$$

Here, we have used the result that $D_{kl}^{i}Y_{nm}^{j}(\mathbf{r})$ at $r=0$ is nonzero only for $i=j$, $n=k$, and $m=l$, and that its value for this special case is $1/\epsilon_{nm}$. Also, in deriving the above result we have assumed that the monopoles at $\mathbf{x}^c$ and $\mathbf{x}^p$, are equal, i.e., $A_{00}^{0,c}=A_{00}^{0,p}$, a result that is verified *a posteriori* from Eq. (17). Thus, the term containing τ^{-1} in Eq. (4) made no contribution to Eq. (17). Finally, we also made use of the following result for the integration of generalized functions:

$$\int_V Y_{nm}^{j}(\mathbf{r})\mathscr{D}_{kl}^{i}\delta(\mathbf{r}-\mathbf{r}^{cp})dV=(-1)^k\mathscr{D}_{kl}^{i}Y_{nm}^{j}(\mathbf{r}^{cp}). \tag{18}$$

Expression (17) allows one to compute the multipoles at $\mathbf{x}^p$ given their values at $\mathbf{x}^c$. A more convenient form that is useful for computing these multipoles can be obtained by using the results given in Appendix A where we have presented more detailed formulae for evaluating the derivatives of spherical harmonics.

It may be noted that the first few multipoles at $\mathbf{x}^p$ could also be obtained by a straightforward Taylor series expansion of C^c around $\mathbf{x}^p$. Thus, using

$$\mathscr{G}S_1(\mathbf{r}-\mathbf{r}^{cp})=\mathscr{G}S_1(\mathbf{r})-\mathbf{r}^{cp}\cdot\nabla\mathscr{G}S_1(\mathbf{r})+\ \ldots, \tag{19}$$

the relations among first few multipoles can be readily obtained

$$A_{00}^{0,p}=A_{00}^{0,c},\quad A_{10}^{0,p}=A_{10}^{0,c}-r_1^{cp}A_{00}^{0,c},$$
$$A_{11}^{0,p}=A_{11}^{0,c}+r_2^{pc}A_{11}^{0,c},\ \ldots. \tag{20}$$

It is easy to verify that these are in agreement with the more general result given by Eq. (17). Calculations of higher-order multipoles using the Taylor series expansion, however, becomes cumbersome and the method presented here based on generalized functions proves more convenient.

To complete the translation, we need to determine the constant e^p. For this purpose we start with the identity

$$\int_V\left[C-\frac{1}{6}r^2\nabla^2C\right]dV=\frac{1}{3}\int_{\partial V}\mathbf{n}\cdot\left[\mathbf{r}C-\frac{1}{2}r^2\nabla C\right]dA \tag{21}$$

and once again substitute for C in turn both C^p and C^c. The volume V is chosen to be the basic unit cell in which both $\mathbf{x}^c$ and $\mathbf{x}^p$ lie and ∂V is the surface of the unit cell. Since both C^p and C^c are required to be equivalent at all points on the surface of the unit cell, the surface integral in both cases must be identical leading thereby to the equality of the volume integrals

$$\int_\tau\left[C^c-\frac{1}{6}r^2\nabla^2C^c\right]dV=\int_\tau\left[C^p-\frac{1}{6}r^2\nabla^2C^p\right]dV. \tag{22}$$

Substituting for C^c and C^p, noting that the integral of $\mathscr{G}S_1$ over the unit cell vanishes, and using the generalized function representation of Laplacians of C^c and C^p, we obtain

$$e^p+\frac{2\pi}{3\tau}A_{20}^{0,p}=\frac{2\pi}{3\tau}[A_{00}^{0,c}\mathbf{r}^{pc}\cdot\mathbf{r}^{pc}-2A_{10}^{0,c}r_1^{pc}+2A_{11}^{0,c}r_2^{pc}+2A_{11}^{1,c}r_3^{pc}+A_{20}^{0,c}], \tag{23}$$

which can be further simplified by substituting for $A_{20}^{0,p}$ from Eq. (17) to obtain

$$e^p=\frac{2\pi}{\tau}[A_{00}^{0,c}\{(r^{pc})^2-Y_{20}^{0}(\mathbf{r}^{pc})\}+3(A_{11}^{0,c}r_2^{pc}+A_{11}^{1,c}r_3^{pc})] \tag{24}$$

Equations (17) and (24) allow us to shift the multipole singularities at point $\mathbf{x}^c$ to that at $\mathbf{x}^p$. These will be useful in combining the disturbance created a group of particles γ into an equivalent disturbance created at a single point $\mathbf{x}^p$.

2. Translation of regular solutions

We now consider the problem of translating a field $C^{\mathrm{reg},p}$ which is regular at both $\mathbf{x}^p$ and $\mathbf{x}^c$ (these are not to be confused with the singular points we used in the previous derivation) and for which a spherical harmonic expansion around $\mathbf{x}^p$ is known to the corresponding field with its expansion around $\mathbf{x}^c$. Let

$$C^{\mathrm{reg},p}=-\frac{1}{6}fr^2+\sum_{j,n,m}E_{nm}^{j,p}Y_{nm}^{j}(\mathbf{r}) \tag{25}$$

be the regular expansion around $\mathbf{r}=\mathbf{x}-\mathbf{x}^p=\mathbf{0}$. We then wish to determine the coefficients that appear in the expansion around $\mathbf{x}^c$

$$C^{\mathrm{reg},c}=-\frac{1}{6}f|\mathbf{r}-\mathbf{r}^{cp}|^2+\sum_{i,k,l}E_{kl}^{i,c}Y_{kl}^{i}(\mathbf{r}-\mathbf{r}^{cp}). \tag{26}$$

For this purpose we use the fact that E_{kl}^{i} is related to a kth order derivative of $C^{\mathrm{reg},c}$ evaluated at $\mathbf{r}=\mathbf{r}^{cp}$

$$E_{kl}^{i,c}=\epsilon_{kl}\mathscr{D}_{kl}^{i}\left[C^{\mathrm{reg}}+\frac{1}{6}f|\mathbf{r}-\mathbf{r}^{cp}|^2\right]_{\mathbf{r}=\mathbf{r}^{cp}}. \tag{27}$$

Substituting for C^{reg} from Eq. (25) we obtain the desired result

$$E_{kl}^{i,c}=\frac{1}{6}f\epsilon_{kl}[\mathscr{D}_{kl}^{i}\{(r^{cp})^2-2\mathbf{r}\cdot\mathbf{r}^{cp}\}]_{\mathbf{r}=\mathbf{r}^{cp}}+\epsilon_{kl}\sum_{j,n,m}E_{nm}^{j,p}\mathscr{D}_{kl}^{i}Y_{nm}^{j}(\mathbf{r}^{cp}). \tag{28}$$

Once again, expressions for the first few coefficients $E_{kl}^{i,c}$ could also be obtained using the Taylor series expansion, and the results obtained that way can be shown to be in agreement with the above more general result.

C. An $O(N)$ algorithm

We now describe the $O(N)$ algorithm for computing the Laplace interactions. This consists of the following steps:

(1) *Create a hierarchy tree.* The first step is to create a hierarchy among groups of particles. For simplicity, we shall assume that our basic unit cell is cubic. We divide this into 8 equal-sized cubes each with its linear dimension half that of the basic cell. These are referred to as the level 0 boxes. Next, each box at level 0 is further subdivided into 8 smaller level 1 boxes leading to a total of 64 boxes at level 1. The process is continued to the finest level m_{lev} at which the box size is such that on average there are P particles per finest level box, P being a constant of $O(1)$ whose precise value must be determined by optimizing the total computational time. Note that there are a total of $m_{\text{lev}}+1=\log_8(N/P)$ levels. Finally, each particle is assigned the finest level ''parent'' box in which its center lies.

(2) *Upward pass.* The second step is to determine the multipole representation of the fields induced by a group of particles that is valid at large distance from the group. It is assumed that we shall determine the multipoles of the particles by a suitable iterative procedure [cf. Step (5)]. Thus, at the beginning of each iteration we start with the assumed values of the multipoles $A_{nm}^{j,\gamma}$ for each particle and compute the contribution from each particle's multipoles to its parent box multipoles and the constant e^p at m_{lev} level using Eqs. (17) and (24) with $\mathbf{x}^p$ in that expression being the position vector of the center of the parent box and $\mathbf{x}^c$ and $A_{kl}^{i,c}$, respectively, the center and the multipoles of particle γ. Next, with the multipoles and the constant e for all the finest level boxes computed, we determine the multipoles and e for the next coarser $m_{\text{lev}}-1$ level boxes with each parent box multipoles now determined from the multipoles of its eight ''children'' at level m_{lev}. This procedure is repeated to larger size boxes to compute the constant e and the multipoles of all the boxes at all the levels.

(3) *Downward pass.* The multipoles and the constant e determined in Step (2) give the far-field representation of the effects of particles whose center is located in a given box. We next want to compute f and E_{kl}^i, i.e., the coefficients that appear in describing the regular field, for all the boxes at all the levels. This is achieved by starting with the boxes at level 1 (or level 0 if the basic unit cell is not cubic but oblong instead, for example) and determining the contribution to the regular field expansion about the center of the boxes from the disturbance due to particles in the other boxes at the same level but the ones that are not its nearest neighbors. Here, and in the subsequent discussion, we shall refer to all the 26 nearest neighbors of a given box at a given level and the box itself as the nearest neighbor of the box for the sake of brevity. Thus, a given box has 27 nearest neighbors. At level 1, there are $4^3-3^3=37$ boxes that are further away from a given box and contributions to f and E_{kl} of a given box from the particles in these 37 boxes can be determined using Eq. (11) with the summation over γ in that expression replaced by the summation over these 37 ''equal generation'' boxes. Of course, $\mathbf{x}^\alpha$ must be replaced by the position vector of the center of the box whose regular coefficients are being computed and $\mathbf{x}^\gamma$ by the center of the equal generation box from which the contribution is being computed. Also, S to be used equals the net sink S^{eq} due to all the particles represented by the equal generation boxes. This can be determined from Eq. (12) with the summation over γ once again replaced by the summation over the equal generation boxes. Now comparing with the regular expansion given by Eq. (25), we see that at this level f for a given box is the sum of S^{eq} over its 37 equal generation distant neighbors.

Next, we compute f and E_{kl}^i of the boxes at the next finer level, i.e., level 2. Unlike level 1, in addition to the contribution from its equal generation level 2 boxes (there are $6^3-3^3=189$ equal generation boxes for each box at this level), we must also determine the contribution from the regular expansion of its parent box at level 1. Denoting the box at level 2 under consideration by a superscript c, the parent by p, and the equal generation box by eq, we write

$$f^c=f^p+\sum_{\text{eq}} S^{\text{eq}}, \quad E_{kl}^{i,c}=E_{kl}^{i,p\to c}+\sum_{\text{eq}} E_{kl}^{i,\text{eq}\to c}, \tag{29}$$

and use Eq. (28) to determine the contribution from the parent $(p\to c)$; the equal generation contribution to f and E_{kl} is determined, as before, with the use of Eqs. (11) and (12). It should be noted that the parent of a box accounts for the field induced by all the particles lying in the distant boxes of level 1. Thus, for each level 2 box, we have now accounted for all the particles that are outside its nearest 27 level 2 boxes. The particles in these 27 boxes are too close to an arbitrarily selected particle in the box under consideration and therefore we must wait for the calculations of the coefficients for the finer level boxes to account for their effect.

The above procedure of combining contributions from the equal generation boxes and the parent box is continued to levels 3,4, $\ldots, m_{\text{lev}}$. At all these levels, the total number of equal generation boxes from which the contributions are computed equals 189, except for the finest m_{lev} level, for which we sum over all the 216 boxes. This includes additional 27 nearest neighbor boxes with one small difference: the singular part $1/r$ is removed from S_1 before computing the contribution from these nearest 27 boxes. Physically, this accounts for all the particles that are lying in the periodic images of the nearest neighbor boxes at the finest m_{lev} but not the particles in the nearest boxes themselves which are too close to permit the use of far-field representation in determining the regular field expansion. We shall account for these particles separately via Step (4).

Finally, we compute the contribution to f and E_{kl}^i of each particle α from the finest level parent box. There is, of course, no contribution from the equal generation boxes at the particle level.

(4) *Particle to particle contribution.* The contributions from the particles in the nearest 27 boxes are evaluated in the same way as for the contributions from the equal generation boxes in the previous step except that the function $S_1(\mathbf{r})$ is now replaced by $1/r$ because the regular part of S_1 has already been accounted for in Step (3).

(5) *Determine new guess for the multipoles.* The Steps (2)–(4) constitute one iteration in solving for the multipoles

of the particles. A suitable iterative procedure, such as the generalized moment residual (GMRES) method, is used to obtain the new guess for the multipoles.

Steps (2)–(5) must be repeated until the multipoles converge to within a specified accuracy. We now make several remarks regarding the procedure outlined above.

Remark 1. For problems in suspension mechanics, we typically use the periodic boundary conditions. For this special case, creating the hierarchy tree is a trivial matter. Once the basic unit cell is divided into a specified number of levels, this tree remains unchanged throughout the dynamic simulation. In order that this remains computationally efficient, the number of particles in any of the finest level boxes must not become much greater than its average value P. This will be true provided that no isolated cluster with a large number density develop as the simulation proceeds. This is an important consideration in stellar dynamics where the overall number density of particles (stars/planets) is very small and the cluster (galaxy) formation is an important phenomenon to be investigated through simulations. In such a case, m_{lev} may have to be changed during the simulations and may not remain uniform throughout the basic cell. The computational effort for the determination of the tree for such highly nonuniform systems scales as $N(\log N)^4$ as shown by Aluru and co-workers.[27,28] The number density of particles in most suspension problems is typically large and the probability of developing a highly nonuniform suspension is generally small. In few exceptional cases, such as gas–solid fluidized bed where large voids devoid of any particles may form, creating tree with nonuniform m_{lev} may prove useful.

Remark 2. If the multipole moments representing the effect of groups of particles are computed up to $n=N_{sp}$, the computational effort for the upward pass scales as $(N_{sp}+1)^4N$: there are a total of $(N_{sp}+1)^2$ multipole coefficients to be evaluated and each depend linearly on the same number of multipoles of its children. The computational cost for computing the parent to child contribution to the coefficients E_{kl} in the regular expansion is also $O((N_{sp}+1)^4N)$, assuming that these coefficients are also computed up to $k=N_{sp}$. The cost of computing the contribution from the equal generation boxes is roughly $216/P$ times that for the parent to child calculation, P being the average number of particles per box. Finally, the particle to particle contribution requires an $O(27P(N_s+1)^4N)$ effort. Here, N_s is the order of multipoles retained in describing the field induced by the particles. Thus, as a first approximation, the total computational cost per one iteration is controlled by the equal generation contribution and the particle to particle contribution. A rough estimate of the total operation count is therefore $[216(N_{sp}+1)^4/P+27P(N_s+1)^4]N$ and this has a minimum for $P=3[(N_{sp}+1)/(N_s+1)]^2$. Of course, this is to be used only as a rough guide to estimate how optimum P might depend on N_s and N_{sp}. More accurate estimate can be obtained through numerical experimentation.

The total operation count and the estimate of optimum P obtained here are different from that of Greengard and Rokhlin[12] who used a slightly more complex algorithm which scales as N_{sp}^3 instead of the fourth power dependence obtained in the present algorithm. Similar reduction in the exponent of N_{sp} is obtained in a related calculation by Zinchenko.[29] These investigators considered very high values of N_{sp} for which the reduction is significant. As will be shown in Sec. IV, a very good accuracy is obtained even with N_{sp} as small as 3 and therefore we have not implemented their method here.

Remark 3. If the dimension of the unit cell does not change in dynamic simulations, then it is possible to save considerable computational time by storing various matrices that are needed in computing the parent to child or child to parent contributions, and the contribution from the equal generation boxes. In particular, the only place where one needs to use Ewald's technique for determining S_1 and its derivatives is in the equal generation computations and these calculations need to be done only once, at the beginning of the simulations. Also the total number of derivatives to be evaluated is $O(4N_{sp}^2\log N)$, which amounts to a negligible cost compared with a total derivatives of $O(4N_s^2N^2)$ that one must evaluate at *every* time step in the $O(N^2)$ algorithm described in the previous section.

III. THE METHOD FOR STOKES INTERACTIONS

Having described in detail the method for Laplace interactions, we now consider the method for Stokes interactions. The basic idea is same as before and we need to address only two important issues: (i) how to include the lubrication effects such that reasonably accurate particle trajectories are obtained with very few unknowns per particle; and (ii) how to translate the singular and regular solutions of Stokes equations. Of course, the lubrication effects could also be important in some problems involving Laplace interactions, e.g., the problem of determining the effective thermal conductivity of dense suspensions consisting of highly conducting inclusions, but we chose to defer the discussion of the issue (i) to the present section to explain the important aspects of the algorithm through a relatively simple problem for which the lubrication effects are absent.

We shall follow the method of Sangani and Mo[8] to account for the lubrication forces in Stokes flow. This method separates the force density on the surface of the particles into a singular distribution of the force density near the narrow gap between the particles and a regular distribution of force density over the entire surface of the particles. The singular force density gives asymptotically correct forces on the particles in terms of their velocities and the gap width while the regular distribution is expanded in the case of spherical particles in a series of multipoles at the center of the particles, and their values are determined by satisfying the boundary condition on the surface of the particles. In addition to giving correct lubrication forces and torques on the particles in close proximity, the method also accounts for the effect of the velocity induced by the lubrication forces on the other particles in the suspension. The velocity of the fluid is given by

$$u_i(\mathbf{x})=\langle u_i\rangle(\mathbf{x})+\sum_{\alpha=1}^{N}\mathscr{M}_j^{\alpha}v_{ij}(\mathbf{x}-\mathbf{x}^{\alpha})+u_i^{\mathrm{lub}}(\mathbf{x}), \tag{30}$$

where $\langle u_i \rangle$ is the average velocity of the suspension, v_{ij} is a spatially periodic Green's function for the Stokes equation, $\mathscr{M}_j^\alpha$ is a differential operator, and u_i^{lub} is the velocity induced by the lubrication force density. Detailed expressions for each of these quantities may be found in Mo and Sangani[7] and Sangani and Mo.[8] In particular, $-(F_j/4\pi\eta)v_{ij}(\mathbf{r})$ is the velocity at $\mathbf{r}$ due to point forces $\mathbf{F}$ acting at the lattice points of the periodic array. As shown by Hasimoto,[25]

$$v_{ij}=S_1\delta_{ij}-\frac{\partial^2 S_2}{\partial r_i \partial r_j}, \tag{31}$$

where S_1 is the same function as introduced earlier in the Laplace interaction calculations, and S_2 satisfies $\nabla^2 S_2 = S_1$. $v_{ij}(\mathbf{r})$ has a singular behavior near $r=0$ as given by

$$v_{ij}\to v_{ij}^s \equiv \frac{1}{r}-\frac{1}{2}\frac{\partial^2 r}{\partial r_i \partial r_j}, \tag{32}$$

the well-known Oseen tensor for the flow induced due to a point force at origin in a fluid at rest at infinity. The actual expression for the differential operator $\mathscr{M}_j^\alpha$ is somewhat involved but, fortunately, will not be needed for our discussion. The only thing that we need to note is that it is defined such that, when operated on v_{ij}^s, it produces terms that coincide with the singular terms in the Lamb's general solution in terms of spherical harmonics. More specifically, let the velocity of the fluid near the surface of particle α be expanded in the Lamb's solution as

$$\mathbf{u}^\alpha = \mathbf{u}^{s,\alpha}+\mathbf{u}^{r,\alpha} \tag{33}$$

with $\mathbf{u}^{s,\alpha}$ and $\mathbf{u}^{r,\alpha}$ being, respectively, the singular and regular parts of $\mathbf{u}$ at $\mathbf{x}=\mathbf{x}^\alpha$. These are defined by

$$\mathbf{u}^{s,\alpha}(\mathbf{r})=\sum_{n=1}^{\infty}\left[c_n^s r^2\nabla p_n^{s,\alpha}+b_n^s \mathbf{r} p_n^{s,\alpha}+\nabla\mathbf{x}(\mathbf{r}\chi_n^{s,\alpha})+\nabla\phi_n^{s,\alpha}\right], \tag{34}$$

where $\mathbf{r}=\mathbf{x}-\mathbf{x}^\alpha$,

$$c_n^s=\frac{2-n}{2n(2n-1)}, \quad b_n^s=\frac{n+1}{n(2n-1)}, \tag{35}$$

and p_n^s, χ_n^s, and ϕ_n^s are spherical harmonics of degree $-n-1$. (For this section we temporarily suppress our previous notation according to which ϕ is the volume fraction of the particles.) We define the above spherical harmonics in terms of ''multipole'' coefficients P_{nm}^j, etc., by means of

$$\begin{aligned} p_n^{s,\alpha}&=\sum_{m,j} P_{nm}^{j,\alpha} Y_{nm}^j r^{-2n-1},\\ \chi_n^{s,\alpha}&=\sum_{m,j} T_{nm}^{j,\alpha} Y_{nm}^j r^{-2n-1},\\ \phi_n^{s,\alpha}&=\sum_{m,j} \Phi_{nm}^{j,\alpha} Y_{nm}^j r^{-2n-1}, \end{aligned} \tag{36}$$

where the summation over m is from 0 to n and for j from 0 to 1. Likewise, the regular part is written as

$$\mathbf{u}^{r,\alpha}(\mathbf{r})=\sum_{n=1}^{\infty}\left[c_n^r r^2\nabla p_n^{r,\alpha}+b_n^r \mathbf{r} p_n^{r,\alpha}+\nabla\mathbf{x}(\mathbf{r}\chi_n^{r,\alpha})+\nabla\phi_n^{r,\alpha}\right], \tag{37}$$

with $c_n^r=c_{-n-1}^s$, $b_n^r=b_{-n-1}^s$, and

$$\begin{aligned} p_n^{r,\alpha}&=\sum_{m,j} P_{nm}^{rj,\alpha} Y_{nm}^j,\\ \chi_n^{r,\alpha}&=\sum_{m,j} T_{nm}^{rj,\alpha} Y_{nm}^j,\\ \phi_n^{r,\alpha}&=\sum_{m,j} \Phi_{nm}^{rj,\alpha} Y_{nm}^j. \end{aligned} \tag{38}$$

In Mo and Sangani,[7] we have defined the differential operator $\mathscr{M}_j^\alpha$ in terms of the coefficients $P_{nm}^{j,\alpha}$, etc., that appear in Eqs. (36) such that

$$u_i^{s,\alpha}=\mathscr{M}_j^\alpha v_{ij}^s, \tag{39}$$

where v_{ij}^s is the Oseen tensor [cf. Eq. (32)]. We also gave expressions for evaluating the coefficients that appear in the regular part of the velocity at $\mathbf{x}^\alpha$ in terms of the singular coefficients $P_{kl}^{i,\gamma}$, etc., of all the particles in the suspension. This is analogous to the expression we cited for the Laplace interactions [cf. Eq. (11)] except that the corresponding expressions for the Stokes interactions are considerably more involved. The direct evaluation of these regular coefficients requires an $O(N^2)$ computational effort. In the present section we shall derive the results for the translation of regular and singular solutions that will allow us to determine the regular coefficients with an $O(N)$ effort.

A. Translation of Stokes singularities

We wish to translate $u_i^c=\mathscr{M}_j^c v_{ij}(\mathbf{x}-\mathbf{x}^c)$ with its singularities at $\mathbf{x}^c$ to a velocity field with its singularities at $\mathbf{x}^p$ such that both are equivalent at a point $\mathbf{x}$ sufficiently far away from both $\mathbf{x}^c$ and $\mathbf{x}^p$. Since the field with singularities at $\mathbf{x}^p$ must also be spatially periodic, the most general form for it is given by

$$u_i^p=e_i+\mathscr{M}_j^p v_{ij}(\mathbf{x}-\mathbf{x}^p), \tag{40}$$

where e_i is a constant. Let p^c and p^p be the corresponding pressure fields. Substituting p for C in Eq. (14) we obtain

$$\int_V Y_{nm}^j(\mathbf{r})\nabla^2 p^c \, dV_{\mathbf{r}}=\int_V Y_{nm}^j(\mathbf{r})\nabla^2 p^p \, dV_{\mathbf{r}}, \tag{41}$$

where $\mathbf{r}=\mathbf{x}-\mathbf{x}^p$. Now since the pressure satisfies the Laplace equation except at its singularities, the integrals in the above expression can be evaluated simply from the singular behavior of p which can be written as

$$p^s=\eta\sum_{k,l,i} P_{kl}^i Y_{kl}^i r^{-2k-1}=\eta\sum_{k,l,i}\lambda_{kl}^{-1} P_{kl}^i \mathscr{D}_{kl}^i r^{-1}, \tag{42}$$

where we have made use of Eq. (A1) in writing the last equality. Noting that $\nabla^2 r^{-1}=-4\pi\delta(\mathbf{r})$, it is relatively easy to carry out integrations in Eq. (41) to obtain a relation similar to Eq. (17)

$$P_{nm}^{j,p}=\epsilon_{nm}\lambda_{nm}\sum_{i,k,l}\lambda_{kl}^{-1}P_{kl}^{i,c}\mathscr{D}_{kl}^{i}Y_{nm}^{j}(\mathbf{r}^{pc}), \tag{43}$$

where $\mathbf{r}^{pc}=\mathbf{x}^{p}-\mathbf{x}^{c}$.

Now we determine $T_{nm}^{j,p}$. Let $\omega=\nabla\times\boldsymbol{u}$ be the vorticity. Using Eqs. (34) and (35), it can be shown that the singular part of the vorticity is given by

$$\omega^{s,a}=\sum_{n}\ -\frac{1}{n}\mathbf{r}^{a}\times\nabla p_{n}^{s,a}-n\nabla\chi_{n}^{s,a}-\mathbf{r}^{a}\nabla^{2}\chi_{n}^{s,a}, \tag{44}$$

where the superscript a stands for c as well as p, and $\mathbf{r}^{a}=\mathbf{x}-\mathbf{x}^{a}$. Now we note that $\mathbf{r}\cdot\omega^{a}$ satisfies the Laplace equation at all points except at its singular point $\mathbf{x}^{a}$. This can be seen by multiplying Eq. (44) with $\mathbf{r}$ and using $\mathbf{r}^{a}=\mathbf{r}-\mathbf{r}^{ap}$ to yield

$$\mathbf{r}\cdot\boldsymbol{\omega}^{s,a}=\sum_{n}\ -\frac{1}{n}\mathbf{r}^{ap}\cdot(\mathbf{r}\times\nabla p_{n}^{s,a})+[n(n+1)-n\mathbf{r}^{ap}\cdot\nabla -r^{2}\nabla^{2}+\mathbf{r}^{ap}\cdot\mathbf{r}\nabla^{2}]\chi_{n}^{s}. \tag{45}$$

Taking Laplacian of the above equation and using results such as $\mathbf{r}^{a}\cdot\nabla\chi_{n}^{s,a}=-(n+1)\chi_{n}^{s,a}$ (since $\chi_{n}^{s,a}$ is a homogeneous polynomial of degree $-n-1$ in r_{i}^{a}) and $\mathbf{r}=\mathbf{r}^{a}+\mathbf{r}^{ap}$ we obtain

$$\nabla^{2}(\mathbf{r}\cdot\boldsymbol{\omega}^{s,a})=\sum_{n}\ -\frac{1}{n}\mathbf{r}^{ap}\cdot\mathbf{r}\times\nabla\nabla^{2}p_{n}^{s,a}+[n^{2}+5n+6 -(n+2)\mathbf{r}^{ap}\cdot\nabla+\mathbf{r}\cdot(\mathbf{r}^{ap}-\mathbf{r})\nabla^{2}]\nabla^{2}\chi_{n}^{s,a}. \tag{46}$$

Now substituting $\mathbf{r}\cdot\omega$ for C in Eq. (14), using the generalized function representation of Laplacians of p_{n}^{s} and χ_{n}^{s}, and simplifying the resulting integrals we obtain

$$\frac{n(n+1)}{\lambda_{nm}\epsilon_{nm}}T_{nm}^{j,p}=\sum_{k,l,i}\frac{1}{\lambda_{kl}}\Bigg[k(n+1)T_{kl}^{i,c}\mathscr{D}_{kl}^{i}Y_{nm}^{j}+\frac{1}{k}P_{kl}^{i,c}\mathbf{r}\cdot\{\mathscr{D}_{kl}^{i}(\mathbf{r}\times\nabla Y_{nm}^{j}(\mathbf{r}))\}\Bigg]_{\mathbf{r}=\mathbf{r}^{pc}}. \tag{47}$$

This can be further simplified using the general results for differentiation of spherical harmonics given in Appendix A. A convenient set of formulas for computing all the multipoles at $\mathbf{x}^{p}$ from those at $\mathbf{x}^{c}$ is given in Appendix B.

To compute the coefficients $\Phi_{nm}^{j,p}$ we start with the identity

$$\frac{\partial}{\partial x_{j}}(\sigma_{ij}u_{i}'-\sigma_{ij}'u_{i})=u_{i}'\frac{\partial\sigma_{ij}}{\partial x_{j}}+p'\frac{\partial u_{i}}{\partial x_{i}}, \tag{48}$$

where $\sigma_{ij}\equiv-p\,\delta_{ij}+\eta(\partial u_{i}/\partial x_{j}+\partial u_{j}/\partial x_{i})$ is the stress tensor corresponding to a field (u_{i},p) and σ_{ij}' is the stress corresponding to a regular field (u_{i}',p'). (u_{i},p) on the other hand, is allowed to be singular at some points in the space. We now choose the regular fields to be given by

$$p'=Y_{nm}^{j}(\mathbf{r}),\quad \mathbf{u}'=c_{n}^{r}r^{2}\nabla Y_{nm}^{j}+b_{n}^{r}\mathbf{r}Y_{nm}^{j}, \tag{49}$$

substitute for $(\mathbf{u},p)$ both $(\mathbf{u}^{c},p^{c})$ and $(\mathbf{u}^{p},p^{p})$ in turn, integrate the identity (48) over a volume V large enough to contain both $\mathbf{x}^{c}$ and $\mathbf{x}^{p}$, apply the divergence theorem, and use the equivalence of the two fields at all points on the boundary ∂V to obtain

$$\int_{V}[\{c_{n}^{r}r^{2}\nabla Y_{nm}^{j}(\mathbf{r})+b_{n}^{r}\mathbf{r}Y_{nm}^{j}(\mathbf{r})\}\cdot(\nabla\cdot\boldsymbol{\sigma}^{c})+Y_{nm}^{j}(\mathbf{r})\nabla\cdot\mathbf{u}^{c}]dV_{\mathbf{r}} =\int_{V}[\{c_{n}^{r}r^{2}\nabla Y_{nm}^{j}(\mathbf{r})+b_{n}^{r}\mathbf{r}Y_{nm}^{j}(\mathbf{r})\}\cdot(\nabla\cdot\boldsymbol{\sigma}^{p}) +Y_{nm}^{j}(\mathbf{r})\nabla\cdot\mathbf{u}^{p}]dV_{\mathbf{r}}. \tag{50}$$

Since the divergence of stress and velocity are zero except at the singular points, only the singular part of the velocity and stress will contribute to the above integrals. Substituting the singular part of the velocity for u_{i}^{a}, where a stands for c or p, the integrands in the above expression reduce to

$$\sum_{k}\Bigg[\Bigg\{\frac{1}{k}(c_{n}^{r}r^{2}\nabla Y_{nm}^{j}+b_{n}^{r}\mathbf{r}Y_{nm}^{j})\cdot\mathbf{r}^{a}+c_{k}^{s}(r^{a})^{2}Y_{nm}^{j}\Bigg\}\nabla^{2}p_{k}^{s} +(c_{n}^{r}r^{2}\nabla Y_{nm}^{j}+b_{n}^{r}\mathbf{r}Y_{nm}^{j})\cdot(\nabla\times(\mathbf{r}^{a}\nabla^{2}\chi_{k}^{s}))+Y_{nm}^{j}\nabla^{2}\phi_{k}^{s}\Bigg]. \tag{51}$$

Using the generalized function representation of Laplacians of p_{k}^{s}, etc., and carrying out the integrations in Eq. (50) we obtain

$$\Phi_{nm}^{j,p}=\epsilon_{nm}\lambda_{nm}\sum_{i,k,l}\Bigg[\Phi_{kl}^{i,c}\mathscr{D}_{kl}^{i}Y_{nm}^{j}+\frac{1}{n+1}T_{kl}^{i,c}\mathbf{r}^{pc}\cdot\nabla\times(\mathscr{D}_{kl}^{i}(\mathbf{r}Y_{nm}^{j}))+P_{kl}^{i,c}\Bigg\{\Bigg(c_{n}^{r}+c_{k}^{s}-\frac{1}{k(n+1)}\Bigg)\times\mathscr{D}_{kl}^{i}(r^{2}Y_{nm}^{j})+\Bigg(\frac{1}{k(n+1)}-\frac{2-k}{k(2k-1)}\Bigg)\mathbf{r}\cdot\mathscr{D}_{kl}^{i}(\mathbf{r}Y_{nm}^{j})+\frac{2-k}{2k(2k-1)}r^{2}\mathscr{D}_{kl}^{i}Y_{nm}^{j}\Bigg\}\Bigg]_{\mathbf{r}=\mathbf{r}^{pc}}. \tag{52}$$

A convenient formula for evaluating Φ_{nm}^{j} based on the above expression is given in Appendix B.

Finally, to complete the transformation of the singular solution at $\mathbf{x}^{c}$ to that at $\mathbf{x}^{p}$, we need to determine the constant e_{i} in Eq. (40). For this purpose we use the identity

$$\int_{\tau}[\mathbf{u}^{c}-\mathbf{r}\nabla\cdot\mathbf{u}^{c}]dV=\int_{\tau}[\mathbf{u}^{p}-\mathbf{r}\nabla\cdot\mathbf{u}^{p}]dV=\int_{\partial\tau}\mathbf{r}\mathbf{u}\cdot\mathbf{n}\,dA, \tag{53}$$

where τ is the unit cell enclosing both $\mathbf{x}^{c}$ and $\mathbf{x}^{p}$ and $\mathbf{n}$ is a unit outward normal on its surface $\partial\tau$. As before, we have used the equivalence of $\mathbf{u}^{c}$ and $\mathbf{u}^{p}$ on $\partial\tau$. Since v_{ij} and its derivatives are solenoidal, and since their integrals over the unit cell vanish, substituting for $\mathbf{u}^{c}$ and $\mathbf{u}^{p}$ [cf. Eq. (40)] yields $\mathbf{e}=\mathbf{0}$.

B. Translation of regular solutions of Stokes equations

We now consider a solution of Stokes equation which is regular both at $\mathbf{x}^p$ and $\mathbf{x}^c$ and for which the coefficients $(P_{nm}^{rj,p}, T_{nm}^{rj,p}, \Phi_{nm}^{rj,p})$ in the regular Lamb's solution around $\mathbf{x}^p$ are known. Our goal is to derive expressions for its expansion around $\mathbf{x}^c$, i.e., to determine the coefficients $P_{nm}^{rj,c}, T_{nm}^{rj,c}$ and $\Phi_{nm}^{rj,c}$. Since the pressure satisfies the Laplace equation, the coefficients in its expansion are related by the same expression as for E_{kl} in Sec. II [cf. Eq. (28) with $f=0$]

$$P_{kl}^{ri,c} = \epsilon_{kl} \sum_{j,n,m} P_{nm}^{rj,p} \mathscr{D}_{kl}^{i} Y_{nm}^{j}(\mathbf{r}^{cp}). \tag{54}$$

Similarly, we use the fact that $\boldsymbol{\omega}^r \cdot \mathbf{r}$ with $\mathbf{r} = \mathbf{x} - \mathbf{x}^c$ satisfies the Laplace equation and obtain

$$\begin{aligned} k(k+1) T_{kl}^{ri,c} &= \epsilon_{kl} (\boldsymbol{\omega}^r \cdot \mathbf{r})_{\mathbf{r}=\mathbf{0}} \\ &= \epsilon_{kl} \sum_{j,n,m} \left[k(n+1) T_{nm}^{rj,p} \mathscr{D}_{kl}^{i} Y_{nm}^{j}(\mathbf{r}^{cp}) - \frac{1}{n+1} \right. \\ &\quad \left. \times P_{nm}^{rj,c} \{ \mathbf{r} \cdot (\nabla (\mathscr{D}_{kl}^{i} (\mathbf{r} Y_{nm}^{j}))) \}_{\mathbf{r}=\mathbf{r}^{cp}} \right]. \end{aligned} \tag{55}$$

Finally, we use the fact that $\mathbf{r} \cdot \mathbf{u}^r$ is biharmonic, and therefore $\Phi_{kl}^{ri,c}$ can be evaluated from[7]

$$\Phi_{kl}^{ri,c} = \frac{\epsilon_{kl}}{k} \left[\left\{ \mathscr{D}_{kl}^{i} - \frac{(k-l)(k-l-1)}{4k-2} \mathscr{D}_{k-2,l}^{i} \nabla^2 \right\} (\mathbf{r} \cdot \mathbf{u}^r) \right]_{\mathbf{r}=\mathbf{r}^{cp}}. \tag{56}$$

Once again, the detailed expressions for determining various coefficients of the regular part of the velocity are given in Appendix B.

C. The $O(N)$ algorithm for Stokes interactions

The $O(N)$ algorithm for Stokes interactions consists of the same steps as outlined in Sec. II. In addition to computing the contribution from the singularity at the center of particle γ to the regular field near particle α, we also calculate the flow induced by the lubrication forces between each pair of particles in close proximity. In Sangani and Mo,[8] we gave the expression for the flow due to lubrication forces in terms of a force dipole singularity situated at the center of the gap between the particles. The upward pass now determines the equivalent force multipoles of the finest level boxes from both the force multipoles of the particles and the lubrication singularities. The remainder of the upward pass calculations in which the multipoles are evaluated for the coarser level boxes remain unaffected by the lubrication singularities. In the downward pass calculations, the contribution from the equal generation boxes is evaluated by the expressions given in Mo and Sangani[7] with the center of particle γ in that study now replaced by the center of the equal generation box, and the center of particle α replaced by the center of the box whose regular coefficients are being evaluated. Finally, in the particle to particle step, we evaluate the contribution from the particles and the lubrication singularities lying in the 27 nearest neighbor boxes. For this we need additional expressions for computing the contribution to coefficients in the regular part of the velocity near each particle from the singularities situated at the center of the particles and the lubrication gaps. These expressions are given in Appendix B.

IV. APPLICATION TO FEW SPECIFIC SUSPENSION PROBLEMS

In this section we apply the method described in the previous two sections to few specific problems with the aim of assessing the utility of the method in studying systems with large N. Since the computational effort increases as N_{sp}^4, we shall be particularly interested in determining the accuracy of the method for smaller N_{sp}.

To validate the analytical results for computing the translation of singular and regular solutions of Laplace and Stokes equations, and to test the accuracy of the computer programs, we found it very useful to compare the results of the programs against $O(N^2)$ programs which were extensively tested previously for their accuracy.[7,8,18,24] Since the computational time required by these $O(N^2)$ algorithms is very large, the accuracy for large N was tested by arranging the N particles within the basic unit cell in a periodic array with each sub-unit cell containing N_0 particles. Typically, the calculations were checked with $N_0=1$, which corresponds to a truly periodic array, and with $N_0=16$, the particles within the sub-unit cell arranged in the latter case in a random array. Since in the $O(N^2)$ method we compute each element of the matrix $\mathbf{A}$ separately and then evaluate the product $\mathbf{A} \cdot \mathbf{x}$, the most important test of the $O(N)$ algorithm requires the direct evaluation of this product to match with the corresponding product evaluated by the $O(N^2)$ method for any given $\mathbf{x}$. Here, for example, for the case of Laplace interactions, $\mathbf{x}$ is the vector of $A_{nm}^{i,\gamma}$ while the product is the vector of $E_{kl}^{j\alpha}$ [cf. Eq. (11)] plus a constant times the vector of $A_{kl}^{j,\alpha}$, with the constant depending on the boundary condition at the surface of the particles. The elements of the matrix $\mathbf{A}$ being related to the derivatives of S_1 evaluated at $\mathbf{x}=\mathbf{x}^\alpha - \mathbf{x}^\gamma$. Taking $A_{nm}^{i,\gamma}=1$ for all n,m,i, and γ, we evaluate the mean value of $E_{kl}^{j,\alpha}$ over all the particles and its variance from the mean. For the special case of a periodic array with $N_0=1$, the variance must, of course, be zero. However, the $O(N)$ algorithm with finite N_{sp} introduces some fluctuations even in the case of a periodic array. These fluctuations were found to decrease rapidly with the increase in N_{sp}. The mean value for each E_{kl} was also found to agree well with that obtained from the $O(N^2)$ algorithm as we shall show in more detail below. Similar tests were also made for the Stokes interactions code.

A. Laplace interactions

A few typical results for the relative errors for the special case of diffusion-controlled reactions are given in Table I. The boundary condition on the surface of particles for this problem yields Eq. (7). Denoting the left-hand side (lhs) of this equation by $r_{nm}^{i,\alpha}$ we calculate two measures of the relative errors. The first is defined by

$$E_1 = \frac{1}{n_{\text{eq}}} \sum_{n,m,i} \left| \frac{\langle r_{nm}^{i,\alpha} \rangle - \langle \overline{r_{nm}^{i,\alpha}} \rangle}{\langle \overline{r_{nm}^{i,\alpha}} \rangle} \right|, \tag{57}$$

TABLE I. Relative errors from the Laplace interaction code as a function of N_{sp} for different values of N_s. Case A: simple cubic array with $\phi=0.3$, $N_0=1$, $N=512$. Case B: random array with $\phi=0.25$, $N_0=16$, $N=1024$.

Case	N_s	N_{sp}	E_1	E_2
A	1	1	4.0E-2	1.3E-3
		2	4.0E-2	1.3E-3
		4	7.5E-4	2.1E-4
A	2	2	7.9E-2	1.1E-2
		4	7.4E-2	1.1E-2
		5	9.5E-5	2.2E-4
B	1	1	2.5E-2	1.1E-2
		2	1.1E-1	1.9E-2
		4	1.4E-1	1.3E-1
		5	1.9E-3	2.5E-3
B	2	2	8.0E-2	4.9E-2
		4	7.8E-2	2.2E-2
		5	6.9E-4	9.9E-3

where the angular brackets denote the average over all the particles in the unit cell, $r_{nm}^{i,\alpha}$ is the lhs of Eq. (7) computed by the $O(N)$ algorithm, $\overline{r_{nm}^{i,\alpha}}$ is the corresponding value obtained from the $O(N^2)$ algorithm, and $n_{\text{eq}}=(N_s+1)^2$ is the total number of unknowns per particle, N_s being the highest order multipole used in describing the disturbance field due to each particle ($n\leqslant N_s$). The order of multipoles to which the disturbance created by groups of particles is represented in the $O(N)$ algorithm is denoted by N_{sp}.

The second measure of the relative error is

$$E_2=\frac{1}{n_{\text{eq}}}\sum_{n,m,i}\left|\frac{\langle E_{nm}^{i,\alpha}\rangle-\langle\overline{E_{nm}^{i,\alpha}}\rangle}{\langle\overline{E_{nm}^{i,\alpha}}\rangle}\right|, \tag{58}$$

where $E_{nm}^{i,\alpha}$ is computed using the $O(N)$ algorithm and $\overline{E_{nm}^{i,\alpha}}$ by the $O(N^2)$ algorithm. This error is a true representation of the error introduced by the grouping of particles and is relatively insensitive to the volume fraction ϕ of particles. The error E_1 on the other hand, depends on the specific boundary condition and is therefore dependent on the nature of problem to be solved. Also since the magnitude of $E_{nm}^{i,\alpha}$ decreases relative to the coefficient of the singular term $A_{nm}^{i,\alpha}$ as the volume fraction decreases, this error will decrease as ϕ is decreased.

As seen in Table I both relative errors are generally small in magnitude even though the errors do not decrease monotonically with N_{sp}. For the special case of periodic arrays with $N_0=1$, only the multipoles A_{nm} with n and m multiples of 4 are nonzero and therefore a significant reduction in the error is expected to occur only when N_s and N_{sp} are incremented by 4. This is found to be generally true even for random arrays. In most cases the errors for $N_{sp}=N_s+4$ are seen to be very small, well within the accuracy of the $O(N^2)$ algorithm.

Table II shows the computing time for one iteration on a single IBM SP2 processor at the Cornell Theory Center. The times shown there are for an interactive calculation on the machine and thus represent approximate times. They are useful, however, for illustrating the dependence of computer time on N, N_s, N_{sp}, and P. We see that the computing time

TABLE II. Computing time (in s) per iteration using a single processor on IBM SP2: eq gen, pp, and total refer to time for computing equal generation contribution, particle to particle contribution, and the total time, respectively. (These times are for the diffusion-controlled reaction problem.)

N	m_{lev}	N_s	N_{sp}	eq gen	pp	Total
512	2	1	1	2.0	0.7	2.8
		1	2	3.6	0.7	4.6
		1	4	47.6	0.7	49.2
		2	2	3.6	2.6	6.6
		2	5	113	2.7	117
1024	2	0	0	1.7	0.5	2.3
		1	1	2.7	3.4	6.4
		1	2	3.6	2.7	6.8
		1	3	7.2	2.7	11.0
		1	4	49	2.7	54
		3	3	7.1	31	40
		4	4	50	73	128
4096	3	1	1	21.5	5.5	28
		1	4	375	5.5	387
		2	2	38	21	62
		4	4	386	145	550
8192	3	1	1	23	23	48

is essentially governed by the downward pass in which the evaluation of the contributions from the equal generation neighbors and the particle to particle interactions to the regular coefficients $E_{kl}^{i,\alpha}$ take up most of the computing time. As mentioned earlier, the operation count for the equal generation roughly scales as $216N(N_{sp}+1)^4/P$, and that for the particle to particle as $27NP(N_s+1)^4$. The scaling of these times with N_{sp}, N_s, and P can be verified approximately from the data presented in Table II. For example, the particle to particle time quadrupoled when N was increased from 512 to 1024 keeping $N_s=1$. Note that with $m_{\text{lev}}=2$, there are 512 boxes and hence P equals, respectively, 1 and 2 for $N=512$ and 1024. Similarly, the particle to particle time changed roughly by a factor of 4 when N_s was changed from 1 to 2 at $N=512$. The ratio of particle to particle time to the equal generation time is somewhat variable. For $N_s=N_{sp}$ the ratio of this time does approximately scale as P^2, but the ratio appears to vary considerably with N_s ranging from 0.07 for $N_s=0$ and $N=512$ to 1.09 for $N_s=N_{sp}=3$ and $N=1024$. This variation may be partly due to inaccurate nature of the timing obtained from the interactive calculations. More importantly, however, the difference may arise because the particle to particle calculations require evaluation of spherical harmonics for each pair of particles whereas the calculation for the equal generation contribution uses precalculated derivatives of S_1.

The set of equations given by Eq. (7) were solved iteratively using a subroutine based on the generalized minimum residual method for nonsymmetric matrices written at Lawrence Livermore. The routine determines the approximate solution $\mathbf{x}^{\text{ap}}$ to $\mathbf{A}\cdot\mathbf{x}=\mathbf{b}$ and generates an estimate of the error defined as the square root of Euclidian norm of the difference $\mathbf{b}-\mathbf{A}\cdot\mathbf{x}^{\text{ap}}$ divided by the norm of $\mathbf{b}$. Since it is not known *a priori* what error estimate is acceptable for generating a satisfactory solution to a given problem, we must

TABLE III. Convergence of the reaction rate $\mathscr{R}_s$ as a function of number of iterations (iter) and N using a generalized residual moment (GMRES) algorithm. Error refers to the error estimate calculated by the GMRES code and var$=\langle A^2-\langle A\rangle^2\rangle/\langle A\rangle^2$ is the non-dimensional variance in the induced monopoles, $A\equiv A_{00}^0$.

N	ϕ	$N_s=N_{sp}$	Iter	Error	$\mathscr{R}_s$	var
1024	0.1	2	6	5.8E-2	2.08	3.8E-2
			11	8.1E-3	2.11	4.1E-2
			17	9.5E-4	2.11	4.2E-2
			23	7.0E-5	2.11	4.2E-2
		0	12	9.7E-3	2.06	8.4E-2
1024	0.3	2	10	6.0E-1	4.74	1.3E-2
			20	4.5E-2	4.95	1.6E-2
			38	9.2E-5	4.95	1.6E-2
4096	0.3	1	20	1.7E-1	4.15	3.3E-1
			40	1.0E-2	4.19	3.7E-1
4096	0.01	1	8	8.9E-3	1.19	4.6E-2
			24	1.0E-5	1.19	4.6E-2
8192	0.1	1	9	1.5E-1	1.89	4.1E-2
			19	9.7E-3	2.00	4.1E-2

TABLE IV. A comparison of the results for the non-dimensional diffusion-controlled reaction rate $\mathscr{R}_s$ and the monopole variance (cf. Table III caption) obtained by the $O(N^2)$ and $O(N)$ algorithms.

		$O(N^2)$			$O(N)$			
ϕ	N_0	N_s	R_s	var	N	N_{sp}	R_s	var
0.45	1	0	9.06	0.0	512	0	8.35	0.0
					512	4	9.06	0.0
					4096	0	6.03	1.1E-5
					4096	4	9.05	1.7E-9
		4	10.31	0.0	512	4	10.31	0.0
					4096	4	10.30	1.0E-7
		8	10.31	0.0				
0.45	16	1	9.98	2.5E-3	1024	2	8.71	3.3E-3
						4	9.98	2.5E-3
		2	10.74	1.7E-3		2	9.37	3.0E-3
		3	11.17	1.7E-3		3	9.50	1.7E-3
		4	11.33	1.7E-3		4	11.39	1.5E-3
0.1	16	0	2.17	2.6E-2	1024	0	1.65	3.4E-2
		1	2.31	1.7E-2		1	2.31	1.8E-2
		2	2.34	1.7E-2		2	2.31	1.8E-2
		3	2.34	1.7E-2		3	2.27	1.6E-2

study the convergence properties for various problems separately.

1. Diffusion-controlled reactions

We begin with the diffusion-controlled reactions. Here, our primary interest is in determining the non-dimensional reaction rate $\mathscr{R}_s$. This is determined as follows.

It can be shown that the average concentration is related to C^∞ in Eq. (3) by

$$\langle C\rangle = C^\infty - \phi\left[\frac{1}{2}\langle A_{00}^{0,\alpha}\rangle + \frac{1}{15}S\right], \tag{59}$$

where the angular brackets denote average over all the particles, ϕ is the volume fraction of the particles, S is the strength of sink [cf. Eq. (2)], and $A_{00}^{0,\alpha}$ is the strength of induced monopole due to the presence of particle α, the radius of the spheres being taken to be unity. The non-dimensional reaction rate can be shown to be given by

$$\mathscr{R}_s = \frac{S(1-\phi)}{3\phi\left[C^\infty + \frac{S}{6}\left(1-\frac{2}{5}\phi\right)\right]}. \tag{60}$$

For computing $\mathscr{R}_s$, we take $C^\infty=1$ and first determine $A_{00}^{0,\alpha}$. S is then determined from the overall heat balance which gives $S=-3\phi\langle A_{00}^{0,\alpha}\rangle$. Finally, substituting for S in Eq. (60) yields $\mathscr{R}_s$.

An additional quantity that gives some measure of the convergence is the variance in the monopole strength from its average value. Table III gives both $\mathscr{R}_s$ and the variance for various values of ϕ and N. In all cases the convergence is seen to be quite rapid, with the number of iterations for a given error estimate increasing slowly with N.

Table IV shows a comparison between the results obtained by the $O(N^2)$ and $O(N)$ algorithms. First, we find that the convergence of $\mathscr{R}_s$ with N_s is very rapid. Thus, a reasonably high accuracy is achieved with N_s less than or equal to 4 even at high volume fractions. For the special case of a periodic array ($N_0=1$), the results obtained here are in agreement with the results reported by Felderhof.[22] As mentioned earlier, we expect a very high accuracy from the $O(N)$ algorithm when $N_{sp}=N_s+4$. This is indeed the case. However, even the results obtained with lower values of N_{sp} are seen to introduce only a modest error, typically less than 10%.

In studying large systems it will be desirable to carry out simulations with the lowest order approximation that keeps the essential physics of the problem. In the present case, this corresponds to $N_s=1$. The net reaction rate is related to the monopoles ($n=0$) and the effective diffusivity of the medium is governed by the induced dipoles ($n=1$). Since the concentration on the surface of the particles is specified (viz., $C=0$), we expect a Brinkman-like screening of the conditionally averaged concentration. More specifically, it is easy to show that the average concentration $\langle C\rangle_1$ at $\mathbf{x}$ given a sphere at $\mathbf{x}_1$ satisfies $\nabla^2\langle C\rangle_1=\alpha^2\langle C\rangle_1$ for large $\mathbf{r}\equiv\mathbf{x}-\mathbf{x}_1$ with $\alpha^2=3\phi\mathscr{R}_s D/(D^*(1-\phi))$, D^* being the effective diffusivity in reacting media and is analogous to the Brinkman viscosity used in describing the conditional averaged velocity in the analogous case of Stokes flow through an array of fixed particles. For large r, we therefore expect $\langle C\rangle_1-\langle C\rangle$ to decay as $e^{-\alpha r}/r$, the radius of the particles being taken to be unity. Thus, the conditional average concentration decays algebraically as $1/r$ for small r and exponentially for r larger than the screening length $1/\alpha$. For small ϕ, this screening length is of $O(\phi^{-1/2})$, and a question we would like to address is if such a screening can be observed clearly in simulations based on $O(N)$ algorithms with small N_{sp} or do the imposed lengths due to hierarchial division of the suspension interfere with the screening phenomenon.

Figure 1 shows the conditionally averaged monopole as a function of r. The ordinate $\mathscr{M}$ is defined by

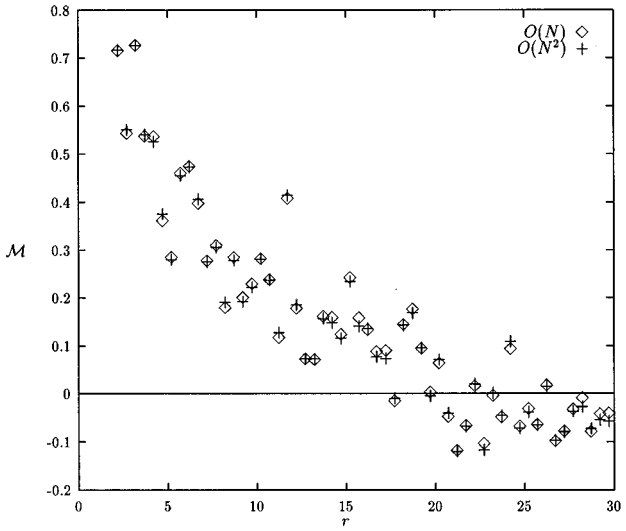

FIG. 1. The normalized conditionally averaged monopole $\mathscr{M}$ as a function of r in a system with $N=512$ and $\phi=0.01$. The $O(N)$ calculations were done with $N_s=N_{sp}=1$ and the $O(N^2)$ with $N_s=1$.

$$\mathscr{M}=r\frac{\langle A\rangle-\langle A\rangle_1(r)}{\langle A\rangle}, \tag{61}$$

where $\langle A\rangle$ is the average monopole ($\langle A_{00}^{0,\alpha}\rangle$) and $\langle A\rangle_1(r)$ is the average of the monopoles of particles separated by distance r. Is is easy to show that the conditionally averaged monopole is proportional to the conditionally averaged concentration $\langle C\rangle_1$ and therefore we expect $\mathscr{M}$ to decay as $e^{-\alpha r}$ for distances large compared with unity but small compared with the size of the unit cell. The calculations were done for a single configuration of 512 randomly placed particles with $\phi=0.01$, $N_s=1$, and $N_{sp}=1$. The same configuration was used also for evaluating $\mathscr{M}$ using the $O(N^2)$ algorithm so that a detailed comparison of the conditional averaged monopoles can be made. The agreement between the two is remarkably good for all values of $r\leqslant 30$. The unit cell size was about 60 units and with the two hierarchial levels used in the $O(N)$ calculations, the box sizes at the first and second levels were, respectively, 15 and 7.5 units. As seen in Fig. 1, there appears to be no influence of these lengths on the results obtained with the $O(N)$ method even for N_{sp} as small as unity.

It is interesting to make a comparison of the computing times for the two algorithms. For the case mentioned above, the time per iteration was about 3 s and it took 10 iterations to converge. Thus the total time using the $O(N)$ algorithm is about 30 s. The time required by the $O(N^2)$ algorithm on the other hand, was about 4350 s. (Both these times are for interactive calculations on a single IBM SP2 processor.) This consisted of about 2880 s for evaluating various derivatives of S_1. (There are $512\times 511/2=130{,}816$ pairs of particles and for each pair we need to evaluate 9 derivatives of S_1 using the Ewald's technique, which in turn requires sums over a total of 400 real and reciprocal space lattice vectors.) The time for filling the coefficients of matrix took 77 s, and the time solving the system of 2048 equations using a Gaussian elimination method took 1388 s. Note that the total time is dominated by the time for evaluating the derivatives of S_1, a step that is not required in the $O(N)$ algorithm since the derivatives needed for this calculation are precalculated and stored for subsequent calculations. Moreover, as mentioned earlier one needs to evaluate only $O(216\log N)$ number of derivatives as opposed to the $O(N^2)$ derivatives required by the $O(N^2)$ algorithm.

TABLE V. Results for the added mass coefficient C_a.

ϕ	N_0	N_s	C_a	N	N_{sp}	C_a
0.25	1	1	2.00	512	1	2.00
		3	2.03		3	2.03
		5	2.03			
0.45	1	1	3.45	512	1	3.45
		3	3.80		3	3.80
		5	3.82		5	3.82
		7	3.82			
0.25	16	1	2.06	1024	1	2.06
					5	2.06
		3	2.12		3	2.12
		5	2.13			

2. Added mass coefficient

We now consider another problem of Laplace interactions, viz., inviscid, irrotational flow past spheres. This has important applications in understanding the flows of bubbly liquids at large Reynolds numbers and small Weber numbers[19] as well as the acoustic behavior of suspensions.[24] Dynamic simulations for large systems will be needed for understanding the nature of instabilities in bubbly liquids. Here, we shall consider the problem of determining the added mass coefficient of suspended particles. Thus, we determine the resulting inviscid, irrotational flow when all the particles are given a velocity of unit magnitude along the x_1-axis. The velocity of the liquid can be expressed in terms of a velocity potential φ by $\mathbf{u}=\nabla\varphi$, with the continuity equation for the liquid requiring $\nabla^2\varphi=0$. The boundary condition on the surface of the particle α gives $\mathbf{n}\cdot\nabla\varphi=\mathbf{n}\cdot\mathbf{v}^\alpha$, $\mathbf{n}$ being the unit outward normal on the surface of the particle α and $\mathbf{v}^\alpha$ its velocity. With φ near the particle α expanded in spherical harmonics as in Eq. (6), the boundary condition yields

$$nE_{nm}^{i,\alpha}-(n+1)A_{nm}^{i,\alpha}a^{-2n-1}=\delta_{n1}\delta_{m0}\delta_{i0}. \tag{62}$$

Finally, the velocity of the suspension averaged over the whole unit cell is specified to be zero. The added mass coefficient C_a is related to the x_1-component of the impulse I_1 by

$$\langle I_1\rangle\equiv-\rho\left\langle\int_{S^\alpha}\varphi n_1\,dA\right\rangle=-m\langle E_{10}^{0,\alpha}+A_{10}^{0,\alpha}a^{-3}\rangle=(m/2)C_a, \tag{63}$$

where ρ is the density of the liquid and m is the mass of liquid having the same volume as the particle, i.e., $m=(4\pi a^3\rho)/3$.

The results for the added mass coefficient are shown in Table V. The convergence of C_a with N_s is very rapid with

$N_s=1$ giving reasonably accurate estimates. The results obtained using the $O(N)$ algorithm with $N_{sp}=1$ and $N_s=1$ also appear to be quite accurate. The accuracy in this case is better than the reaction-diffusion problem.

B. Stokes interactions

We now consider the applications to Stokes flows past spherical particles. For this case the no-slip boundary condition on the surface of the particles yields a set of relations among the coefficients of singular and regular terms given by[7]

$$\Phi_{nm}^{ri,\alpha}+\frac{(n+1)a^{-2n+1}}{n(2n-1)(2n+1)}P_{nm}^{i,\alpha}+\frac{a^2}{2(2n+1)}P_{nm}^{ri,\alpha}=\Phi_{nm}^{i,\infty}, \tag{64}$$

$$\Phi_{nm}^{i,\alpha}-\frac{a^2}{2(2n+1)}P_{nm}^{i,\alpha}+\frac{na^{2n+3}}{(n+1)(2n+1)(2n+3)}P_{nm}^{ri,\alpha} =P_{nm}^{i,\infty}, \tag{65}$$

$$T_{nm}^{ri,\alpha}+a^{-2n-1}T_{nm}^{i,\alpha}=T_{nm}^{i,\infty}, \tag{66}$$

where the quantities on the right-hand side of the above equations depend on the imposed flow and the translational and rotational velocities of the particles. In addition to the above, we have 6 additional equations per particle for the suspension problems for which the translational and rotational velocities are to be determined given the force and torque acting on the particles [cf. Eqs. (67)–(68)]. As pointed out by Cichoki *et al.*[9] and Cichoki and Hinsen,[30] the accuracy of the numerical results for dense suspensions depend critically on the manner in which the above set of equations is truncated. We follow the truncation scheme used by Mo and Sangani,[7] and solve only the set of equations obtained by truncating Eq. (64) to $n\leqslant N_s$, Eq. (65) to $n\leqslant N_s-2$, and Eq. (66) to $n\leqslant N_s-1$. Likewise, the unknowns are truncated as follows: $P_{nm}^{i,\alpha}$ to $n\leqslant N_s$, $\phi_{nm}^{i,\alpha}$ to $n\leqslant N_s-2$, and $T_{nm}^{i,\alpha}$ to N_s-1. This truncation scheme is based on the asymptotic analysis of the resulting equations at small volume fraction of particles in flow through periodic arrays of spheres by Sangani and Acrivos.[31] For high volume fractions it was found that significantly better results are obtained if additional terms arising for $\Phi_{nm}^{i,\alpha}$ with $N_s-2<n\leqslant N_s$ are also included by substituting $\Phi_{nm}^{i,\alpha}=a^2P_{nm}^{i,\alpha}/(4n+2)$ for $n>N_s-2$. This corresponds to satisfying Eq. (65) without the $P_{nm}^{ri,\alpha}$ term. According to this truncation scheme then we have a total of $3N_s^2-1$ unknown multipoles per particle plus the six components of translational and rotational velocities. The coefficients of regular terms are truncated as follows: $P_{nm}^{ri,\alpha}$ and $\Phi_{nm}^{ri,\alpha}$ with $n\leqslant N_s$ and $T_{nm}^{ri,\alpha}$ with $n\leqslant N_s-1$. Similarly, all the moments of groups of particles in the upward pass and all the coefficients of the regular terms in the Lamb's solution during the downward pass are evaluated in the same way as the above regular coefficients for the particles with N_s replaced by N_{sp}.

As in the case of Laplace equations, the code was tested by comparing the coefficients of all the regular terms obtained by the $O(N)$ algorithm against that obtained from the $O(N^2)$ algorithm developed earlier by Mo and Sangani[7] and a very good agreement between the two was found. We now present results for few specific cases with the primary aim of assessing the accuracy of the method for relatively small N_s and N_{sp}, and the efficiency of the GMRES method for solving the system of equations arising in suspension mechanics.

TABLE VI. The non-dimensional drag coefficient $K=\langle F\rangle/(6\pi\eta Ua)$ for flow through an array of fixed spherical particles.

ϕ	N_0	N_s	$K(O(N^2))$	N	N_{sp}	$K(O(N))$
0.25	1	2	7.08	512	2	7.46
					3	6.91
					5	7.03
		3	8.97		3	8.70
0.5235	1	3	28.0	512	3	25.0
		5	40.9		5	38.6
		7	41.9			
0.25	16	2	6.18	1024	2	-ve
		3	7.36		3	7.11
0.1	16	2	2.65	1024	2	2.72
		3	2.65		3	2.69

1. Permeability of fixed bed of particles

The results for the average non-dimensional drag $K=\langle F\rangle/6\pi\eta aU$ on the spheres placed in a uniform flow with a superficial velocity U are given in Table VI. The Darcy permeability k of the fixed bed of spheres is related to K by $k=2a^2/(9\phi K)$. We find that the results obtained by the two algorithms are in a reasonably good agreement with each other even with $N_{sp}=N_s$, an exception being the case of random array with $\phi=0.25$ for which $N_s=N_{sp}=2$ gave an unphysical result.

The computing times we reported in Table II were for a single SP2 processor. In Table VII we give the computing times for both Laplace and Stokes interactions using multiple processors running in parallel. Since the GMRES code we used for solving the system of equations was written for a scalar computing, we employed a master-workers model.

TABLE VII. Computing times (in s) for the downward pass calculations in Laplace and Stokes interactions using multiprocessors on IBM SP2.

N	N_s	N_{sp}	W	Laplace	Stokes
512	2	2	1	4.7	21.9
			8	0.7	3.4
	2	3	1	7.7	84.7
			8	1.2	12.3
	3	3	8	1.4	13.7
1024	2	2	1	8.6	32.5
			4	2.4	9.3
			8	1.6	5.0
	3	3	1	20.9	132
			8	3.0	26
4096	2	2	8	6.6	30.2
	3	3	8	13.5	...
8192	2	2	8	10.8	39.3

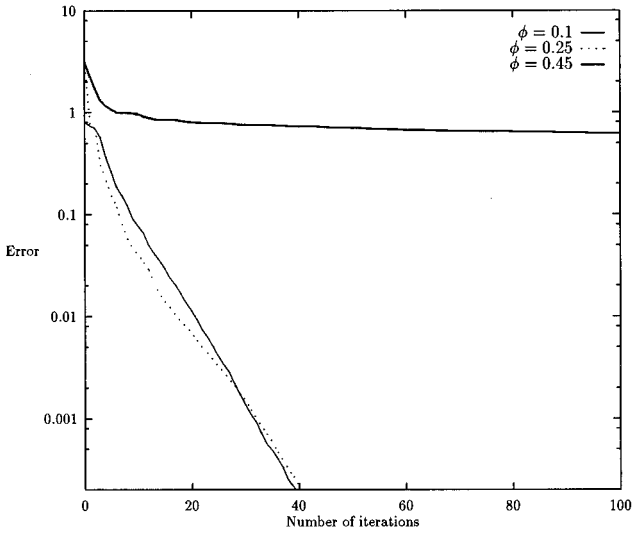

FIG. 2. Error estimate as a function of number of iterations for the permeability problem. $N=512$, $N_s=N_{sp}=2$.

The updating of the unknown multipoles and the upward pass which takes relatively insignificant time were carried out by the master processor who also distributed to all the workers the downward pass (the equal generation and particle to particle) calculations. All the workers essentially used the same memory as the master processor and hence we were limited to systems smaller than about 10,000 particles for $N_s=N_{sp}=2$. We see that the computing time for the downward pass roughly scales linearly with the number of workers W. Also we note that the computing time for the Stokes flow problem is greater than that for the Laplace interaction problem for same values of N_s and N_{sp}. The operation count for Stokes flow interactions for given N_s and N_{sp} can be shown to be slightly less than six times that required for Laplace interactions. This is consistent with the times shown in Table VI which shows the time for Stokes interactions to be roughly 4–5 times that for Laplace interactions. We should note that the computing times shown in Table VI correspond to the case of flow through fixed bed of particles for which the lubrication effects are absent. For the suspension problems to be discussed in the next subsection an additional time will be required for evaluating the contribution from the lubrication velocity field, the magnitude of which depends on the average number of pairs with their center to center distance less than a specified value.

Figure 2 shows the convergence rate for the permeability problem for three different values of volume fraction ϕ for random arrays with $N=512$. The error estimate is defined as before, i.e., the square root of the ratio of Euclidian norm of $\mathbf{A}\cdot\mathbf{x}-\mathbf{b}$ to that of $\mathbf{b}$. The convergence rates for $\phi=0.1$ and 0.25 are nearly equal and much greater than for $\phi=0.45$. Thus, higher values of ϕ will require greater number of iterations. A suitable preconditioning of the matrix may therefore lead to considerable saving in the overall computational times for higher volume fractions. The further work in this direction is left to future work.

2. Effective viscosity and sedimentation

We now consider the problems of determining the effective viscosity of random suspensions of neutrally buoyant particles and the sedimentation velocity of negatively buoyant particles. The calculations for these two problems include the lubrication forces as outlined in Sangani and Mo[8] with two modifications: (i) an expression for the velocity field due to relative motion of two particles in the plane normal to the line joining their centers given in that paper was incomplete and hence needed a correction; and (ii) the torque due to lubrication flow induced by two spheres with unequal rotational velocities omitted in their study was included in the present study. At $\phi=0.45$ we found that this made no more than 5% change in the effective viscosity and thus their influence on the effective viscosity or the sedimentation velocity results presented in Sangani and Mo should be negligible.

For the suspension problems, Eqs. (64)–(66) for the multipoles are supplemented with the additional $6N$ equations given by

$$\mathbf{F}^{\mathrm{reg}}+\mathbf{F}^{\mathrm{lub}}+\mathbf{F}^{\mathrm{ext}}=\mathbf{0}, \tag{67}$$

$$\mathbf{L}^{\mathrm{reg}}+\mathbf{L}^{\mathrm{lub}}=\mathbf{0}, \tag{68}$$

where $\mathbf{F}^{\mathrm{lub}}$ and $\mathbf{L}^{\mathrm{lub}}$ are the lubrication contributions to the force and torque, $\mathbf{F}^{\mathrm{ext}}$ is the external non-hydrodynamic force due to gravity or inter-particle potential, and $\mathbf{F}^{\mathrm{reg}}$ and $\mathbf{L}^{\mathrm{reg}}$ are related to the multipoles P^i_{1m} and T^i_{1m}, respectively [cf. Eqs. (70)–(71) in Mo and Sangani[7]]. The regular parts of the force and torque can be related to the velocity of the particles by considering $n=1$ terms in Eqs. (64) and (66). These are equivalent to the Faxen's laws

$$\mathbf{F}^{\mathrm{reg}}=6\pi\eta a[-\mathbf{v}+\{1+(a^2/6)\nabla^2\}\mathbf{u}^{\mathrm{reg}}],$$

$$\mathbf{L}^{\mathrm{reg}}=4\pi\eta a[-2\boldsymbol{\Omega}+\boldsymbol{\omega}^{\mathrm{reg}}], \tag{69}$$

where $\mathbf{u}^{\mathrm{reg}}$ and $\boldsymbol{\omega}^{\mathrm{reg}}$ are the regular parts of the velocity and vorticity evaluated at the center of the particle.

Initial guess for the velocity of the particles in the case of effective viscosity problem was obtained by solving first Eqs. (67)–(69) with $u_i^{\mathrm{reg}}=\gamma_{ij}x_j$ and $\boldsymbol{\omega}^{\mathrm{reg}}=\nabla\times\mathbf{u}^{\mathrm{reg}}$, γ_{ij} being the imposed shear rate. The solution of these equations converges very quickly, and since only the short-range lubrication forces need to be evaluated, the computational effort is relatively insignificant.

Figure 3 shows the error estimate as a function of the number of iterations using the GMRES code for solving the system of Eqs. (64)–(66) coupled with Eq. (67) and (68) for a random suspension of 512 particles per unit cell. We note that the convergence rates are slower than those obtained in the permeability problem, especially for $\phi=0.1$ and $\phi=0.25$. Thus, the inclusion of lubrication forces decreases the convergence rate. On the other hand, since a good initial guess can be obtained for the viscosity problem by first solving the simple set of equations given by Eqs. (67)–(69), the magnitude of the error is relatively small. Table VIII gives the effective viscosity and the variance in the particles' velocity from the mean as a function of number of iterations. We see that while the error is decreasing slowly with the number of iterations, the values of viscosity and variance obtained even with 40 iterations are reasonably accurate. The

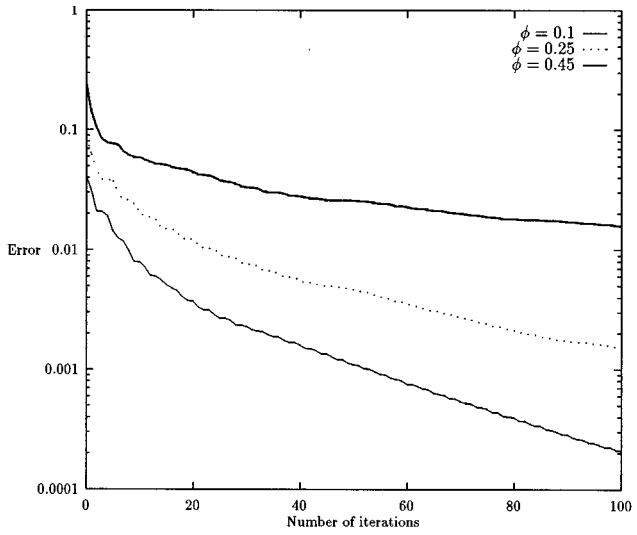

FIG. 3. Error estimate as a function of number of iterations for the effective viscosity problem. $N=512$, $N_s=N_{sp}=2$.

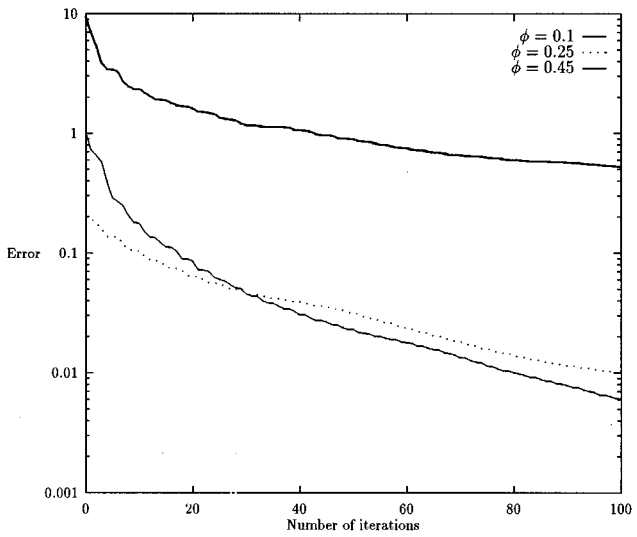

FIG. 4. Error estimate as a function of number of iterations for the sedimentation problem. $N=512$, $N_s=N_{sp}=2$.

effective viscosity does not monotonically converge but oscillates around 5.6, the value reported by Ladd.[6]

The convergence rates for the sedimentation problem are shown in Fig. 4. These rates are very similar to those obtained for the effective viscosity problem. However, unlike the viscosity problem, a good initial guess is difficult to make in the present case, and, consequently, the magnitude of the error is relatively high. On the other hand, the lubrication forces are not very critical in the present problem. Two particles with same external forces sediment together, and the nonzero relative velocity between them can occur only due to the effect of the other particles on $\mathbf{u}^{\mathrm{reg}}$ felt by each particle. This relative velocity is typically small and consequently the lubrication forces play a relatively insignificant role. This can be seen from Table IX which give the results for the sedimentation velocity both with and without the inclusion of lubrication forces. These results were obtained with the $O(N^2)$ algorithm with $N_0=16$. The corresponding results for $N=1024$ particles with the $O(N)$ algorithm were obtained by excluding the lubrication forces for which the error decreases with the number of iterations at a rate similar to that for the permeability problem. We see a generally good agreement between the results obtained by the two algorithms. In view of the fact that the lubrication forces are relatively unimportant, it may be possible to improve the convergence rate without loss of much accuracy by limiting the lubrication forces only between pairs of particles that are very close to each other. The calculations shown in Figs. 3 and 4 included lubrication forces for all pairs of particles with the center to center distance less than $2.6a$. This distance, for example, could be reduced to $2.1a$.

In both suspension problems discussed here the slower convergence rates arise probably due to the fact that some of the coefficients in the force equation (67) are $O(\epsilon^{-1})$ times the velocity difference between the pairs of particles. Perhaps iterative methods in which Eqs. (67)–(69) are solved separately from Eqs. (64)–(66) might lead to better convergence rates. This will be investigated further in a future work.

We close this section by considering sedimentation at a relatively low volume fraction, $\phi=0.05$. Our aim is to check how well the simulations with lower-order approximations,

TABLE VIII. Convergence data for the non-dimensional effective viscosity and particle-velocity variance as functions of number of iterations using the GMRES algorithm: $N=1024$; $N_0=16$; $N_s=N_{sp}=2$. The lubrication contribution is denoted by lub and error is the error estimate obtained by the GMRES code.

ϕ	Iter	Error	η^*/η	lub	var$/(\gamma a)^2$
0.45	40	1.7E-2	5.78	3.4	0.14
	80	1.3E-2	5.57	3.2	0.15
	120	8.0E-3	5.94	3.6	0.16
	160	6.0E-3	5.44	3.1	0.16
0.25	40	3.5E-3	2.10	0.38	0.10
	80	1.3E-3	2.10	0.38	0.10
0.1	40	1.2E-3	1.31	0.048	0.067
	80	3.8E-4	1.31	0.048	0.067

TABLE IX. A comparison of the results for average non-dimensional sedimentation velocity U/U_0 obtained by $O(N)$ and $O(N^2)$ algorithms with $N=1024$ and $N_0=16$. The $O(N^2)$ results are obtained both with and without the lubrication singularities while the $O(N)$ results are obtained without the lubrication singularities.

		$U/U_0(O(N^2))$		$O(N)$	
ϕ	N_s	w lub.	w/o lub.	N_{sp}	U/U_0
0.45	2	0.099	0.100	2	0.057
	3	0.049	0.050	3	0.057
0.25	2	0.173	0.174	2	0.165
	3	0.145	0.146	3	0.151
0.1	2	0.399	0.401	2	0.391
	3	0.388	0.389		

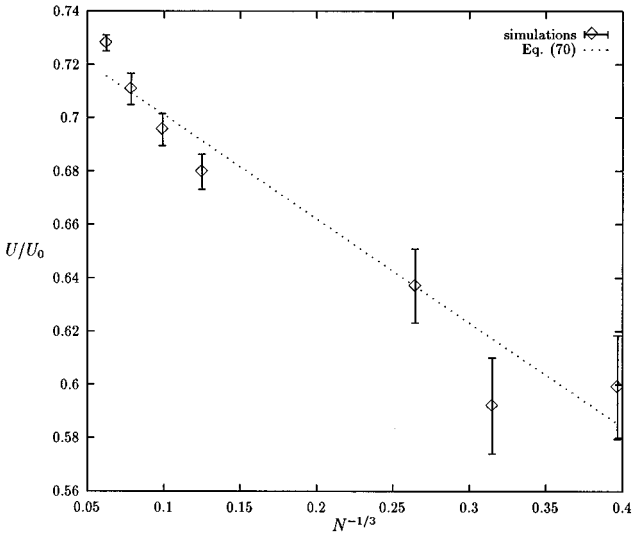

FIG. 5. The non-dimensional average sedimentation velocity as a function of $N^{-1/3}$ for $\phi=0.05$. U_0 is the terminal velocity for an isolated particle.

e.g., $N_s=N_{sp}=2$, satisfy the theoretical prediction by Caflisch and Luke[32] that the velocity variance in random sedimenting suspensions diverge with the system size. In addition to using the lower-order approximations, we also wanted to test if there would be any serious consequences of not using enough iterations in obtaining the solution by the GMRES code. The results for the average sedimentation velocity and velocity variances in the direction of gravity and in the plane transverse to it are presented in Figs. 5 and 6. Each point was obtained by averaging over 15 independent random configurations. The standard error (i.e., standard deviation divided by the square root of the number of data) for the velocity variances computed with these configurations was generally smaller than the size of symbols used in Fig. 6.

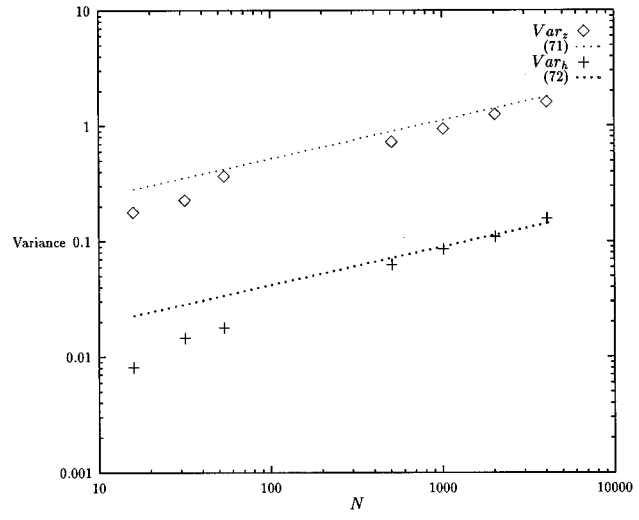

FIG. 6. The divergence of velocity variance with the system size N in random sedimenting suspensions with $\phi=0.05$. The top line corresponds to the theoretical prediction for the velocity variance in the direction of gravity while the bottom line corresponds to the velocity variance in the plane normal to gravity.

The simulations were carried out by requiring that the iterative scheme be terminated either when the error estimate decreases below $5E-4$ or when the number of iterations exceeded 35. For $N=512$ and $N=1024$ the error estimate reached lower than the specified value with an average of 20 and 26 iterations whereas for $N=2048$ and 4096 the truncation was due to number of iterations exceeding 35. The corresponding average error estimates were, respectively, $5.8E-4$ and $2E-3$. These calculations were done noninteractively using 8 SP2 processors. The average time per iteration for the downward pass for $N=4096$ was 25 s, somewhat lower than one reported in Table VII.

In Fig. 5 we have plotted the sedimentation velocity as a function of N. In the limit of large N the sedimentation velocity approaches a constant value as given by (cf. Mo and Sangani[7])

$$U(N)=U^{\infty}-1.7601S(0)U_0\frac{\eta}{\eta^*}\phi^{1/3}N^{-1/3}, \tag{70}$$

where U_0 is the terminal velocity of an isolated particle, U^{∞} is the velocity in an unbounded suspension with finite ϕ, and $S(0)$ is the zero wave number structure factor. For $\phi=0.05$, using $\eta^*/\eta=1.13$ and $S(0)=0.67$ yields the coefficient of $N^{-1/3}$ term in the above equation to equal 0.39. The above relation with $U^{\infty}/U_0=0.74$ is seen to be in a reasonably good agreement with the results of numerical simulations.

Figure 6 shows the results for the velocity variance. Since the long-range interactions are dominated by the fields induced by point forces, one may estimate the variance based on a simple point force approximation. This was done by Ladd[33] who showed that the variance in the velocity component parallel to gravity is given by

$$\mathrm{var}_z\equiv\frac{\langle U_z^2\rangle-\langle U_z\rangle^2}{\langle U_z\rangle^2}=0.823\phi^{2/3}N^{1/3}, \tag{71}$$

and that in the plane normal to gravity by

$$\mathrm{var}_h\equiv\frac{U_h^2}{\langle U\rangle^2}=0.0662\phi^{2/3}N^{1/3}. \tag{72}$$

Thus the velocity fluctuations diverge with N and the fluctuations in the direction parallel to gravity are about 12.4 times that in the plane normal to it. Our simulations are seen to be in excellent agreement with these predictions.

V. CONCLUSIONS

In this paper we have described in detail a method of summing Laplace and Stokes interactions with a computational effort that scales only linearly with the number of particles. The method consists of combining the fields induced by a group of particles in a series of multipoles at the center of the group. The results from the method are in excellent agreement with the ones obtained from previous $O(N^2)$ algorithms as N_{sp}, the order to which the multipole series is expanded, is increased. Very good agreement is obtained in most cases even when N_{sp} equals N_s, the order to which the field induced by the individual particles is represented. The method is combined with the generalized minimum residual

(GMRES) algorithm for solving iteratively the system of linear equations in the multipoles induced by the particles. A number of problems are studied with an aim of assessing the computational time requirements for solving problems in Stokes and Laplace interactions. The method appears to be extremely efficient for solving Laplace interactions. The GMRES algorithm, however, yields a relatively slow convergence rate for the Stokes interaction problems at large volume fractions and further work to improve the convergence rate is desirable. At any rate, the method offers very significant reduction in the overall computational effort over the existing $O(N^2)$ algorithms and may be used for carrying out dynamic simulations of systems of $O(500-10^3)$ particles at very high volume fractions to systems of $O(10^4)$ at low volume fractions.

ACKNOWLEDGMENTS

This work was supported by the National Science Foundation under Grant No. CTS-9307723. All computations were done on the supercomputer facilities at the Cornell Theory Center. The work was inspired by Professor Leslie Greengard's lecture at a workshop organized by the Institute of Mathematics and its Applications (IMA), University of Minnesota in Fall 1994. Sangani gratefully acknowledges the organizers at IMA for the invitation to participate in the workshop.

APPENDIX A: SOME USEFUL FORMULAS FOR THE DIFFERENTIATION OF SPHERICAL HARMONICS

In this appendix, we present some frequently used results concerning differentiation of spherical harmonics. The following result is taken from Hobson:[34]

$$\mathscr{D}^j_{nm} r^{-1} = \lambda_{nm} r^{-2n-1} Y^j_{nm}, \tag{A1}$$

where

$$\lambda_{nm} = (-1)^{n-m}(n-m)!\,2^{1-m}, \tag{A2}$$

$$\mathscr{D}^j_{nm} = \Delta^j_m \frac{\partial^{n-m}}{\partial x_1^{n-m}} \tag{A3}$$

with

$$\Delta^0_m = \left[\left(\frac{\partial}{\partial \xi}\right)^m + \left(\frac{\partial}{\partial \eta}\right)^m\right], \quad \Delta^1_m = i\left[\left(\frac{\partial}{\partial \xi}\right)^m - \left(\frac{\partial}{\partial \eta}\right)^m\right], \tag{A4}$$

and

$$\xi = x_2 + i x_3, \quad \eta = x_2 - i x_3. \tag{A5}$$

The following is also a result from Hobson[34] recast in a slightly different form:

$$\mathscr{D}^i_{kl} Y^j_{nm} = c_1 Y^s_{n-k,m+l} + c_2 Y^s_{n-k,\beta(m-l)}, \tag{A6}$$

with

$$c_1 = (-1)^{ij} 2^{-l} \frac{(n+m)!}{(n-k+m+l)!},$$
$$c_2 = (-1)^{\min}[s' + s\beta(-1)^i] \frac{2^{-l}(n+m)!}{[n-k+\beta(m-l)]!}. \tag{A7}$$

Here, $\min = \min(m,l)$, $\beta = \mathrm{sgn}(m-l)$, $s=1$ if $i+j=1$ and 0 otherwise, and $s'=1-s$. In using Eq. (A7) we must set $Y^s_{pq}=0$ whenever $q>p$. Note that for the special case corresponding to $n=k$, $m=l$, and $i=j$, the above result gives

$$\mathscr{D}^j_{nm} Y^j_{nm} = \epsilon^{-1}_{nm}, \quad \epsilon_{nm} = \frac{(-2)^m}{(1+\delta_{m0})(n+m)!}. \tag{A8}$$

The following identity is useful in evaluating derivatives involving product of two differential operators that appear in expressions such as Eq. (11):

$$\mathscr{D}^i_{kl}\mathscr{D}^j_{nm} = (-1)^{ij}\mathscr{D}^s_{n+k,m+l} + [s' + s\beta(-1)^i](-4)^{-\min} \times \left\{ \mathscr{D}^s_{n+k,\beta(m-l)} - \min \nabla^2 \mathscr{D}^s_{n+k-2,\beta(m-l)} + \frac{\min(\min-1)}{2}\nabla^4 \mathscr{D}^s_{n+k-4,\beta(m-l)} + \cdots \right\} \tag{A9}$$

where the dots represent terms with ∇^6, etc., which are unimportant in most calculations dealing with Laplace and Stokes interaction problems where the functions to be differentiated satisfy either Laplace or biharmonic equation.

The following formula is useful for differentiations involving curl of $\mathbf{r}Y^j_{nm}$:

$$\mathbf{r}\cdot\nabla\times[\mathscr{D}^i_{kl}(\mathbf{r}Y^j_{nm})] = c_3 Y^{s'}_{n-k+1,m+l} + c_4 Y^{s'}_{n-k+1,\beta(m-l)}, \tag{A10}$$

where

$$c_3 = (-1)^{(ij+s)}[-l(n+1)-mk]\frac{2^{-l}(n+m)!}{(n-k+1+m+l)!},$$
$$c_4 = [\beta s' - s(-1)^i][(n+1)l - mk](-1)^{\min} \times \frac{2^{-l}(n+m)!}{[n-k+1+\beta(m-l)]!}. \tag{A11}$$

The other useful results are as follows:

$$\mathbf{r}\cdot\mathscr{D}^i_{kl}(\mathbf{r}Y^j_{nm}) = \frac{2n-k+3}{2n-2k+3} r^2 \mathscr{D}^i_{kl} Y^j_{nm} + d_1 Y^s_{n-k+2,m+l} + d_2 Y^s_{n-k+2,\beta(m-l)}, \tag{A12}$$

$$\mathscr{D}^i_{kl}(r^2 Y^j_{nm}) = 2\mathbf{r}\cdot\mathscr{D}^i_{kl}(\mathbf{r}Y^j_{nm}) + (k-l)(k-l-1) \times \mathscr{D}^i_{k-2,l} Y^j_{nm} - r^2 \mathscr{D}^i_{kl} Y^j_{nm}. \tag{A13}$$

Here,

$$d_1 = (-1)^{ij}\left\{-l + \frac{k(n-k+2-m-l)}{2n-2k+3}\right\} \times \frac{2^{-l}(n+m)!}{(n-k+m+l+1)!}, \tag{A14}$$

$$d_2 = (-1)^{\min} 2^{-l}[s' + s\beta(-1)^i]\left\{-l + \frac{k(n-k+2+m-l)}{2n-2k+3}\right\} \times \frac{(n-k+2-m+l)(n+m)!}{[n-k+2+\beta(m-l)]!}. \tag{A15}$$

APPENDIX B: FORMULAS FOR TRANSLATING SINGULAR AND REGULAR SOLUTIONS OF STOKES EQUATIONS

In this appendix, we present detailed formulas for translating singular and regular solutions of Stokes equations.

Formulas for the upward pass.

$$P_{nm}^{j,p}=\lambda_{nm}\epsilon_{nm}\sum_{i,k,l}\lambda_{kl}^{-1}P_{kl}^{i,c}[c_1Y_{n-k,m+l}^{s}+c_2Y_{n-k,\beta(m-l)}^{s}], \tag{B1}$$

$$T_{nm}^{j,p}=\frac{\lambda_{nm}\epsilon_{nm}}{n(n+1)}\left[\sum_{i,k,l}\frac{T_{kl}^{i,c}}{\lambda_{kl}}k(n+1)\{c_1Y_{n-k,m+l}^{s}+c_2Y_{n-k,\beta(m-l)}^{s}\}+\frac{P_{kl}^{i,c}}{k\lambda_{kl}}\{c_3Y_{n-k+1,m+l}^{s'}+c_4Y_{n-k+1,\beta(m-l)}^{s'}\}\right], \tag{B2}$$

$$\begin{aligned}\Phi_{nm}^{j,p}=\lambda_{nm}\epsilon_{nm}\sum_{i,k,l}\frac{1}{\lambda_{kl}}\Bigg[&\Phi_{kl}^{i,c}\{c_1Y_{n-k,m+l}^{s}+c_2Y_{n-k,\beta(m-l)}^{s}\}-\frac{1}{n+1}T_{kl}^{i,c}\{c_3Y_{n-k+1,m+l}^{s'}+c_4Y_{n-k+1,\beta(m-l)}\}\\&+P_{kl}^{i,c}\left\{\frac{r^2}{4n-4k+6}(c_1Y_{n-k,m+l}^{s}+c_2Y_{n-k,\beta(m-l)}^{s})+c_5Y_{n-k+2,m+l}^{s}+c_6Y_{n-k+2,\beta(m-l)}^{s}\right\}\Bigg],\end{aligned} \tag{B3}$$

where c_1-c_4 are given by Eqs. (A1) and (A11) and

$$\begin{aligned}c_5=\frac{(-1)^{ij}2^{-l}(n+m)!}{(n-k+1+m+l)!}\Bigg[&\left\{\frac{k(n-k+2-m-l)}{(2n-2k+3)}-l\right\}\left(\frac{n+3}{2n+3}-\frac{1}{k}\right)\frac{1}{n+1}+(k-l)(k-l-1)\\&\times\left\{\frac{n+3}{2(n+1)(2n+3)}-\frac{1}{k(n+1)}+\frac{2-k}{2k(2k-1)}\right\}\Bigg],\end{aligned} \tag{B4}$$

$$\begin{aligned}c_6=\frac{(-1)^{\min}2^{-l}(n+m)!}{[n-k+2+\beta(m-l)]!}[s'+s\beta(-1)^{i}]\Bigg[&\left\{\frac{k((n-k+2)^2-(m-l)^2)}{2n-2k+3}-l(n-k+2-m+l)\right\}\left(\frac{n+3}{2n+3}-\frac{1}{k}\right)\frac{1}{n+1}\\&+(k-l)(k-l-1)\left\{\frac{n+3}{2(n+1)(2n+3)}-\frac{1}{k(n+1)}+\frac{2-k}{2k(2k-1)}\right\}\Bigg].\end{aligned} \tag{B5}$$

In the above formulas Y_{pq}^{s} must be evaluated at $\mathbf{x}^p-\mathbf{x}^c$.

Formulas for the downward pass.

Formulas for evaluating contribution to the regular coefficients $P_{kl}^{ri,c}$, $T_{kl}^{ri,c}$, and $\Phi_{kl}^{ri,c}$ from the singularities at the equal generation distant neighbors similar to Eq. (11) may be found in Mo and Sangani.[7] To this the contribution from the parent must be added, the formulas for which are given below

$$P_{kl}^{ri,c}=\epsilon_{kl}\sum_{j,n,m}P_{nm}^{rj,p}[c_1Y_{n-k,m+l}^{s}+c_2Y_{n-k,\beta(m-l)}^{s}], \tag{B6}$$

$$T_{nm}^{ri,c}=\frac{\epsilon_{kl}}{k+1}\sum_{i,k,l}\left[(n+1)T_{nm}^{rj,p}\{c_1Y_{n-k,m+l}^{s}+c_2Y_{n-k,\beta(m-l)}^{s}\}+\frac{P_{nm}^{rj,p}}{k(n+1)}\{c_3Y_{n-k+1,m+l}^{s'}+c_4Y_{n-k+1,\beta(m-l)}^{s'}\}\right], \tag{B7}$$

$$\begin{aligned}\Phi_{kl}^{ri,c}=\epsilon_{kl}\sum_{j,n,m}\Bigg[&\Phi_{kl}^{rj,p}\{c_1Y_{n-k,m+l}^{s}+c_2Y_{n-k,\beta(m-l)}^{s}\}-\frac{1}{k}T_{nm}^{rj,p}\{c_3Y_{n-k+1,m+l}^{s'}+c_4Y_{n-k+1,\beta(m-l)}^{s'}\}\\&+P_{nm}^{rj,p}\left\{\frac{r^2}{4n-4k+6}(c_1Y_{n-k,m+l}^{s}+c_2Y_{n-k,\beta(m-l)}^{s})+c_5Y_{n-k+2,m+l}^{s}+c_6Y_{n-k+2,\beta(m-l)}^{s}\right\}\Bigg].\end{aligned} \tag{B8}$$

The spherical harmonics Y_{nm} in the above expression must be evaluated at $\mathbf{x}^c-\mathbf{x}^p$.

Formulas for particle to particle contribution.

The formulas for determining contribution to the coefficients of regular terms in the expansion around particle α due to singularities at the lubrication point or the neighbor particle γ are obtained from Eqs. (B6)–(B8) by substituting n by $-n-1$. The factorials appearing in these expressions must also be modified. The resulting expressions are given below

$$P_{kl}^{ri,\alpha}=\epsilon_{kl}\sum_{n,m,j,\gamma}\lambda_{nm}^{-1}P_{nm}^{j,\gamma}(g_1+g_2), \tag{B9}$$

$$T_{kl}^{ri,\alpha}=\epsilon_{kl}\sum_{n,m,j,\gamma}\left(-\frac{n}{k+1}\right)\frac{T_{nm}^{j,\gamma}}{\lambda_{nm}}(g_1+g_2)-\frac{1}{nk(k+1)}\frac{P_{nm}^{j,\gamma}}{\lambda_{nm}}(g_3+g_4), \tag{B10}$$

$$\Phi_{kl}^{ri,\alpha}=\epsilon_{kl}\sum_{n,m,j,\gamma}\frac{\Phi_{nm}^{j,\gamma}}{\lambda_{nm}}(g_1+g_2)-\frac{1}{k}\frac{T_{nm}^{j,\gamma}}{\lambda_{nm}}(g_3+g_4)+\frac{P_{nm}^{j,\gamma}}{\lambda_{nm}}\left[\frac{1}{2(1-2n-2k)}r^2(g_1+g_2)+\frac{1}{k}(g_5+g_6)\right], \tag{B11}$$

where

$$g_1=\lambda_{n+k,m+l}(-1)^{ij}r^{-2n-2k-1}Y_{n+k,m}^{s}, \tag{B12}$$

$$g_2=\lambda_{n+k,\beta(m-l)}(-4)^{-\min[s'+s\beta(-1)^i]}r^{-2n-2k-1}Y_{n+k,\beta(m-l)}^{s}, \tag{B13}$$

$$g_3=\lambda_{n+k-1,m+l}(-1)^{ij+s}(nl-mk)r^{-2n-2k+1}Y_{n+k-1,m+l}^{s'}, \tag{B14}$$

$$g_4=\lambda_{n+k-1,\beta(m-l)}(-4)^{-\min[s'-s\beta(-1)^i]}\beta(-nl-mk)r^{-2n-2k+1}Y_{n+k-1,\beta(m-l)}^{s'}, \tag{B15}$$

$$g_5=\lambda_{n+k-2,m+l}(-1)^{ij}r^{-2n-2k+3}Y_{n+k-2,m+l}^{s}\left[(-n-k+1+m+l)\left(\frac{k(2-n)-1+2n}{2n(2n-1)}\right)\left(-2l+2k\frac{n+k+m+l-1}{2n+2k-1}\right)\right.$$
$$\left.-(k-l)(k-l-1)\left(-\frac{1}{n}+\frac{k-2}{4k-2}+\frac{k(n-2)}{2n(2n-1)}\right)\right] \tag{B16}$$

$$g_6=\lambda_{n+k-2,\beta(m-l)}[s'+s\beta(-1)^i](-4)^{-\min}r^{-2n-2k+3}Y_{n+k-2,\beta(m-l)}^{s}\left[(-n-k+1-m+l)\frac{k(2-n)+2n-1}{2n(2n-1)}\right.$$
$$\left.\times\left(-2l+2k\frac{n+k-1-m+l}{2n+2k-1}\right)-(k-l)(k-l-1)\left(-\frac{1}{n}+\frac{k-2}{4k-2}+\frac{k(n-2)}{2n(2n-1)}\right)\right], \tag{B17}$$

where $\mathbf{r}=\mathbf{x}^{\alpha}-\mathbf{x}^{\gamma}$ and Y_{nm}^{s} are evaluated at $\mathbf{r}$.

[1] M. B. Mackaplow, *A Numerical and Experimental Study of Transport Properties of Fiber Suspensions*, Ph. D. thesis, Stanford University 1995.
[2] J. Happel and H. Brenner, *Low Reynolds Number Hydrodyanmics* (Nijhoff, Dordrecht, 1973).
[3] S. Kim and A. J. Karrila, *Microhydrodynamics: Principles and Selected Applications* (Butterworth-Heinemann, London, 1991).
[4] C. Pozrikidis, *Boundary Integral and Singularity Methods for Linearized Viscous Flow* (Cambridge University, Cambridge, 1992).
[5] J. F. Brady and G. Bossis, ''Stokesian dynamics,'' Annu. Rev. Fluid Mech. **20**, 111 (1988).
[6] A. J. C. Ladd, ''Hydrodynamic transport coefficients of random dispersions of hard-spheres,'' J. Chem. Phys. **95**, 3484 (1990).
[7] G. Mo and A. S. Sangani, ''A method for computing Stokes flow interactions among spherical objects,'' Phys. Fluids **6**, 1637 (1994).
[8] A. S. Sangani and G. Mo, ''Inclusion of lubrication forces in dynamic simulations,'' Phys. Fluids **6**, 1653 (1994).
[9] B. Cichoki, B. U. Felderhof, K. Hinsen, E. Wajnryb, and J. Blawzdziewicz, ''Friction and mobility of many spheres in Stokes flow,'' J. Chem. Phys. **100**, 3780 (1994).
[10] A. W. Appel, ''An efficient program for many-body simulation,'' SIAM J. Scientific and Statistical Computing, **6**, 85 (1985).
[11] J. Barnes and P. Hut, ''A hierarchial $O(N \log N)$ force-calculation algorithm,'' Nature (London) **324**, 446 (1986).
[12] L. Greengard and V. Rokhlin, ''A fast algorithm for particle simulations,'' J. Comput. Phys. **73**, 325 (1987).
[13] L. Greengard, ''Fast algorithms for classical physics,'' Science **265**, 909 (1994).
[14] L. Greengard, *The Rapid Evaluation of Potential Fields in Particle Systems* (MIT, Cambridge, MA, 1988).
[15] A. Greenbaum, L. Greengard, and A. Mayo, ''On the numerical solution of the biharmonic equation in the plane,'' Physica D **60**, 216 (1992).
[16] A. J. C. Ladd, ''Numerical simulations of particulate suspensions via a discretized Boltzmann equation. Part 1. Theoretical foundation,'' J. Fluid Mech. **271**, 285 (1994).
[17] A. J. C. Ladd, ''Numerical simulations of particulate suspensions via a discretized Boltzmann equation. Part 2. Numerical results,'' J. Fluid Mech. **271**, 311 (1994).
[18] S.-Y. Kang and A. S. Sangani ''Electrokinetic properties of suspensions of colloidal particles with thin, polarized double layers,'' J. Colloids Interface Sci. **165**, 1637 (1994).
[19] A. S. Sangani and A. K. Didwania, ''Dynamic simulations of flows of bubbly liquids at large Reynolds numbers,'' J. Fluid Mech. **250**, 307 (1993).
[20] M. v. Smoluchowski, ''Versuch einer mathematischen theorie der Koagulationskinetic kolloider Lösungen,'' Z. Phys. Chem. (Leipzig) **92**, 129 (1917).
[21] B. U. Felderhof and J. M. Deutch, ''Concentration dependence of the rate of diffusion-controlled reactions,'' J. Chem. Phys. **64**, 4551 (1976).
[22] B. U. Felderhof, ''Wigner solids and diffusion controlled reactions in a regular array of spheres,'' Physica A **130**, 34 (1985).
[23] A. S. Sangani and C. Yao, ''Bulk conductivity of composites with spherical inclusions,'' J. Appl. Phys. **63**, 1334 (1988).
[24] A. S. Sangani, D. Z. Zhang, and A. Prosperetti, ''The added mass, Basset, and viscous drag coefficients in nondilute bubbly liquids undergoing small-amplitude oscillatory motion,'' Phys. Fluids A **3**, 2955 (1990).
[25] H. Hasimoto, ''On the periodic fundamental solutions of the Stokes equations and their application to viscous flow past a cubic array of spheres,'' J. Fluid Mech. **5**, 317 (1959).
[26] B. Cichoki and B. U. Felderhof, ''Periodic fundamental solution of the linear Navier-Stokes equations.'' Physica A **159**, 19 (1989).
[27] S. Aluru, ''Distribution-independent hierarchial *N*-body methods,'' Ph. D. thesis, Iowa State University, Ames, IA (1994).
[28] S. Aluru, G. M. Prabhu, and J. Gustafson, ''Truly distribution-independent algorithms for the *N*-body problem,'' Proc. Supercomputing '94, 420 (1994). (A full version of this work is submitted to J. Supercomputing.)
[29] A. Z. Zinchenko, ''An efficient algorithm for calculating multiparticle thermal interaction in a concentrated dispersion of spheres,'' J. Comput. Phys. **111**, 120 (1994).
[30] B. Cichoki and K. Hinsen, ''Stokes drag on conglomerates of spheres.'' Phys. Fluids **7**, 285 (1995).
[31] A. S. Sangani and A. Acrivos, ''Slow flow through periodic arrays of spheres,'' Int. J. Multiphase Flow **8**, 343 (1982).
[32] R. E. Caflisch and H. C. Luke, ''Variance in the sedimentation speed of a suspension,'' Phys Fluids **28**, 759 (1985).
[33] A. J. C. Ladd, ''Dynamical simulations of sedimenting spheres,'' Phys. Fluids A **5**, 299 (1993).
[34] E. W. Hobson, *The Theory of Spherical and Ellipsoidal Harmonics* (Cambridge University, Cambridge, 1931).